Multiuser Detection in CDMA MIMO Systems with Timing Mismatch

by

Robert Chao Yung Lu

A thesis submitted to the
Department of Electrical and Computer Engineering
in conformity with the requirements
for the degree of Master of Science (Engineering)

Queen's University
Kingston, Ontario, Canada
January 2004

Abstract

Today, in this information-hungry society, Internet traffic such as multimedia streaming applications is driving the demand for high speed data packet wireless services. The use of multiple transmit and receive antennas has been proposed for the fourth generation code-division multiple access (CDMA) wireless cellular networks in order to meet these demands. Multiuser CDMA multiple-input multiple-output (MIMO) systems have just recently been studied. Receivers proposed for such systems thus far have been based on the assumption that perfect knowledge of the channel state information is available. Although the effects of channel correlation and imperfect estimation on the MIMO system have been rigorously studied, little or no attention has been paid to time-delay mismatch. More importantly, it is well known that timing estimation errors in a CDMA system can result in significant performance degradation, where the near-far resistant property of multiuser detectors is compromised.

In this thesis, we investigate the impact of mismatch in time-delay estimations between transmit-receive antenna pairs in a multiuser CDMA MIMO communication system. We first formulate a robust space-time decorrelator (STD) by decomposing each substream with rectangular chip pulse shapes into two virtual substreams. A multistage successive interference cancellation (SIC) implementation of the robust

STD that requires no ordering is then proposed to reduce complexity and increase capacity. The proposed receiver integrates a receiver diversity combining procedure, residual error estimation, amplitude averaging and soft-decision cancellation to reduce error propagation and noise enhancement. It is demonstrated that the proposed robust space-time SIC (RSTSIC) achieves significant performance improvement over the STD when delay estimation error is present, and its performance is close to that of the STD with perfect timing estimation.

Acknowledgements

I am privileged to have been a member of the Information Processing and Communications Laboratory, which is a very positive environment for learning and working. To this end, I am thankful to all the lab members for the knowledge and friendship shared. Most importantly, I am grateful to Dr. Steven Blostein for his mentorship. I am fortunate to have had a chance to share his enthusiasm in research; his guidance, patience and support are much appreciated.

I would like to acknowledge the members of my thesis committee, Dr. McLane, Dr. Alajaji, Dr. Ibnakahla and Dr. Diak for their invaluable suggestions and comments with respect to this thesis.

This research is in part supported by Canadian Institute for Telecommunications Research (CITR), Graduate Awards from Queen's University, Samsung Electronics, and Bell Canada.

Contents

List of Tables

List of Figures

List of Symbols

a_k	amplitude of user *k*
$a_{k,n}$	amplitude of the *k*th user's *n*th substream
$\overline{a}_{k,n}^{\,j}$	amplitude average at the *j*th iteration
$\hat{a}_{k,n}^{\,j}(m)$	amplitude information collected up to the *j*th iteration
$\tilde{a}_{k,n}^{\,j}(m)$	tentative amplitude information collected up to the *j*th iteration
$\mathbf{A}$	amplitude matrix
$b_k[i]$	*i*th transmitted bit from user *k*
$b_{k,n}(m)$	data bit of the *k*th user's *n*th substream
$\hat{b}_k^j(m)$	*m*th bit estimate for user *k* at the *j*th iteration
$\hat{b}_{k,n}^{\,j}(m)$	data bit estimate at the jth iteration for the *m*th bit of *k*th's users' *n*th substream
$\tilde{b}_{k,n}^{\,j}(m)$	tentative bit estimate at the *j*th iteration for the *m*th bit of *k*th's users' *n*th substream
$\mathbf{b}$	data bit vector
$\hat{\mathbf{b}}$	data bit estimate vector
$\tilde{\mathbf{b}}$	tentative data bit estimate vector
$\hat{\mathbf{b}}(j)$	data bit vector estimate at the *j*th iteration

$\mathbf{B}(z)$	feedback filter
$c_{n,p}$	complex channel coefficient between the *n*th transmit antenna and the *p*th receive antenna
$c_k(l)$	PN code sequence assigned to user *k* at the *l*th chip
$\mathbf{c}_n$	channel vector for the *n*th transmit antenna
$\mathbf{C}$	channel matrix
$\mathbf{C}_p$	N_T-by-N_T diagonal channel matrix at the *p*th receive antenna
$\tilde{\mathbf{C}}_p$	block-diagonal channel matrix of size KMN_T-by-KMN_T at the *p*th receive antenna
$\tilde{\mathbf{C}}'_p$	block-diagonal channel matrix of size $2KMN_T$-by-$2KMN_T$ at the *p*th receive antenna for RSTD
$\tilde{\mathbf{C}}''_p$	block-diagonal channel matrix of size $(M+1)KN_T$-by-$(M+1)KN_T$ at the *p*th receive antenna for multistage RSTD
$\mathbf{C}(j)$	channel matrix at the *j*th iteration
$\mathbf{C}(j)'$	re-ordered channel matrix at the *j*th iteration
$\mathbf{d}$	decision vector
$\mathbf{d}_k$	*k*th user's spreading code vector for the $(M+1)T_S$ second interval
$\mathbf{d}_k(\rho_{n,p}, i)$	$\mathbf{d}_k$ right shifted by $(i-1)L+\rho_{n,p}$ chips
$\mathbf{e}_{k,n,p}$	error vector
$\mathbf{e}^j_{k,n,p}$	error vector at the *j*th iteration
$\mathbf{F}(0)$	spectral-factorized lower triangular matrix
$\mathbf{F}(1)$	spectral-factorized upper triangular matrix with zero diagonal
$\mathbf{G}(z)$	feed-forward filter
$\mathbf{I}_N$	N-by-N identity matrix
K	number of users

L	spreading gain
M	frame size
$n(t)$	AWGN
$n_p(t)$	AWGN on receive antenna *p*
$n(k,i)$	correlation between AWGN and spreading code of *i*th bit of user *k*
$newInfo_{k,n}^{j}(m)$	normalized output after MRC
$newInfo_{k,n,p}^{j}(m)$	matched filter output at the *j*th iteration for the *m*th bit of the *n*th substream of the *k*th user
$\mathbf{n}$	matched filter noise output
$\mathbf{n}_p$	AWGN at the *p*th receive antenna
N_R	number of receive antennas
N_T	number of transmit antennas
$p(t)$	rectangular chip pulse of duration T_C
$r(t)$	received baseband signal
$r_p(t)$	received baseband signal at the *p*th receive antenna
$\mathbf{r}$	received baseband signal vector
$\mathbf{r}_p$	received vector signal at the *p*th receive antenna
$\mathbf{r}_p^j$	stripped composite received signal at the *j*th iteration
$\hat{\mathbf{r}}_{k,n,p}^{j}$	reconstructed received signal at antenna *p* using only the extracted information from the $_j$th iteration for the *k*th user's *n*th substream
$\mathbf{r}(j)$	received signal at *j*th iteration
$\mathbf{R}$	for CDMA system: cross-correlation matrix for MCM system: space-time cross-correlation matrix
$\mathbf{R}(j)$	cross-correlation matrix at the *j*th iteration

$\mathbf{s}_{k,n,p}(i)$	*k*th user's signature waveform for the *i*th interval from the *n*th transmit antenna to the *p*th receive antenna
$\hat{\mathbf{s}}_{k,n,p}(i)$	estimated spreading code vector
$S_k(t)$	normalized spreading code for user *k*
$\mathbf{S}_p$	spreading code matrix at the *p*th receive antenna
$\mathbf{S}'_p$	spreading code vector at the *p*th receive antenna for RSTD
$\mathbf{S}''_p$	spreading code vector at the *p*th receive antenna for multistage RSTD
$\mathbf{S}(z)$	Z-transform of cross-correlation matrix
T_C	chip duration
T_S	symbol duration
$\mathbf{w}$	linear detection transformation
$y_k(i)$	*i*th matched filter output bit of user *k*
$y_k^j(m)$	decision vector for *m*th bit of user *k* at the *j*th iteration
y	matched filter output vector
$\Delta\hat{\mathbf{a}}_{k,n,p}^{\,j}$	amplitude of the error vector at the *j*th iteration
$\Delta\mathbf{r}_{k,n,p}^{\,j}$	residual signal at the *j*th iteration
$\Delta\hat{\mathbf{s}}_{k,n,p}(i)$	error spreading code vector
$\rho(jk,mi)$	spreading code cross-correlation between *m*th symbol of user *j* and *i*th symbol of user *k*
σ^2	AWGN variance
τ_k	time delay of the *k*th user

List of Abbreviations

AMPS	Advance Mobile Phone System
AWGN	Additive White Gaussian Noise
BER	Bit-Error-Rate
BLAST	Bell Labs layered Space-Time
BPSK	Binary Phase-Shift Keyed
CDMA	Code Division Multiple Access
CSI	Channel State Information
GSM	Global System for Mobile
ISI	Inter-Symbol Interference
MAI	Multiple Access Interference
MAP	Maximum-A-Priori
MIMO	Multiple-Input Multiple-Output
MCM	Multiuser CDMA MIMO
ML	Maximum Likelihood
MMSE	Minimum Mean-Squared Error
MRC	Maximal Ratio Combining
MUD	Multi-User Detection
NFR	Near-Far Ratio
PIC	Parallel Interference Cancellation

PN	Pseudo Noise
QoS	Quality of Service
RSTD	Robust Space-Time Decorrelator
RSTSIC	Robust Space-Time Successive Interference Canceller
SIC	Successive Interference Cancellation
SINR	Signal-to-Interference plus Noise Ratio
SISO	Single-Input Single-Output
SNR	Signal-to-Noise Ratio
STD	Space-Time Decorrelator
TDMA	Time Division Multiple Access
TD-SCDMA	Time Division Synchronous Code Division Multiple Access
WCDMA	Wideband Code Division Multiple Access
ZF	Zero-Forcing

Chapter 1

Introduction

Wireless communications is one of the fastest growing industries in history. According to the Canadian Wireless Telecommunications Association, there are 12 million mobile phone users in Canada at the end of year 2002, representing an overall penetration level of approximately 37%. It is projected that, by the year-end 2004, more than half of all Canadians will be mobile phone users. This lucrative business, with revenues totalling over $6 billion in 2001 in Canada alone, has been receiving increasing attention from both the private and public sectors ever since the first launch of wireless networks in the early 1980s.

The first cellular networks were based on analog radio transmission technologies such as AMPS (Advance Mobile Phone System). Busy signals and dropped calls were frequent as the capacities of these networks were quickly becoming saturated with increasing number of subscribers. The Second-generation digital cellular system was drawn up by the industry to cope with increased traffic within a limited amount of bandwidth. One of these technologies, GSM (Global System for Mobile), was introduced in 1991. The new generation of cellular network enjoyed tremendous success, and was quickly adopted worldwide, while another

technology was just emerging. Qualcomm Inc. introduced the IS-95 (Interim Standard-95) in 1993, based on CDMA (code division multiple access) air-interface technology, as an alternative to GSM. The capacity of CDMA claimed to have roughly 18 times more than analog networks, and 4-6 times that of TDMA (time division multiple access), the technology used in GSM [1]. The cellular concept allows the reuse of the same frequency band at different physical locations. Having a frequency reuse factor of 1, i.e., every adjacent cell is allowed to use the same frequency band, CDMA provides the most efficient use of the radio spectrum. Frequency planning, therefore, became obsolete for the CDMA wireless network.

The second-generation of wireless networks were mainly voice-oriented, and the proliferation of the Internet in the mid 1990s led the industry to envision a network that would be capable of delivering high-speed data packets. The International Telecommunications Union adopted three standards for the third-generation (3G) wireless system: CDMA2000, wideband CDMA (WCDMA) and time division synchronous CDMA (TD-SCDMA). The first deployment of 3G systems appeared in Japan in 2001. Commercially today, the CDMA2000 1X network delivers speeds of up to 2.4 Mbps in the indoor environment and a peak data rate of 153.6 Kbps in the mobile environment. The success of the improvements in capacity and data rate of 3G systems can be attributed to technologies such as smart antennas, receiver diversity and selectable mode vocoder.

Anticipating that the wireless networks will have similar Internet usage patterns as that of the wired networks, improvements to the 3G networks were actively pursued by the industry even before the first commercial 3G network was deployed. The fourth-generation wireless networks are envisioned to provide enhanced services with high data rate, and integrated and converged services with IP (Internet protocol)-

based seamless networks [2].

1.1 Multiuser Detection

Spread spectrum is a signal processing technique that distinguishes CDMA, where a data symbol is modulated with a noise-like wideband signal called a pseudo-noise (PN) sequence. This process is also known as spreading, and is intended to suppress multiple access interference (MAI) due to interference from other users in the same cell (intracell-interference), and possibly users from adjacent cells (intercell-interference). The amount of suppression possible in the conventional CDMA receiver, a matched filter, depends on the cross-correlation properties between the PN sequences from all active users and the spreading factor, which is defined as the ratio in bandwidth between the information-bearing signal and the PN sequence. Capacity of the system, therefore, is limited by the available bandwidth and the PN sequence properties. When orthogonal PN sequences are used, however, the capacity becomes solely dependent of the spreading factor.

The matched filter is optimal in a white Gaussian noise environment, but suffers from the near-far effect when MAI is present: the performance of the matched filter deteriorates when the received powers from interfering users are greater than that of the desired user. Stringent power-control is required to avoid the near-far problem, but it is a difficult task in practice.

Multiuser detection, or MUD, seeks to overcome the inherent shortcomings of conventional CDMA receivers by providing near-far resistance for the receiver in the process of eliminating the MAI. An optimum maximum likelihood (ML) MUD receiver was proposed by Verdú [3]. The ML multiuser receiver encompasses a bank

of matched filters that produces a set of sufficient statistics, followed by a Viterbi decoder. The complexity of the ML receiver is exponential in the number of users, rendering it impractical. Suboptimum linear receivers such as the decorrelating and the minimum mean-squared error (MMSE) receivers have been proposed to trade off complexity and performance among the conventional and optimal receivers [4], [5], however, they still require computationally intensive matrix inversion. More practical and simple approaches include multistage decision-feedback receivers such as the parallel interference cancellation (PIC) detector [6], as well as the serial interference cancellation (SIC) detector [7]. Although both receivers have complexity linear in the number of users, the SIC causes longer delay, while the PIC demands more hardware.

All of the above-mentioned multiuser detectors have assumed that the exact signal time-delays of all active users in the same cell are known, which is impossible in practice. Several well-known time delay estimators such as the sliding correlation delay estimator [8], subspace-based estimator [9], [10] and others in [11]-[14] all provide estimation to within 20% of the spreading chip interval or better. Perfect timing estimation, however, cannot be achieved as noise and MAI hinders estimation accuracy. The performances of multiuser detectors under time-delay estimation errors, or timing mismatch, have been studied in [15]-[21]. It is shown that multiuser receivers under timing mismatch are no longer near-far resistant, and under mismatch, MUD receiver performances can even be worse than that of the matched filter.

Thus, new techniques have been proposed to mitigate the devastating effects of timing mismatch in MUD [22]-[25]. The decorrelating-based detectors in [22] and [23] effectively double the number of users, causing increased noise enhancement. As a result, it is shown by analysis that the capacity of these decorrelating receivers is reduced by 50%. Both MMSE-based receivers in [22] and [24] are based on

stochastic delay modelling and both improve the average bit-error-rate (BER), but cannot completely eliminate the MAI introduced by timing mismatch, and, therefore, are not near-far resistant. The robust SIC, proposed by Zha and Blostein [25], is shown to be near-far resistant. Furthermore, the robust SIC has the advantage that the capacity can surpass 50% of the spreading gain, and is of complexity linear in the number of users.

1.2 Multiple-Input Multiple-Output Systems

With increasing demands on current wireless systems put forth by high-speed packet data and multimedia streaming services, technologies that will deliver increased capacity have been of interest to researchers in recent years. While a vast literature is available on increasing user data rate through techniques such as multicode and variable spreading gain, they do so at the expense of reducing the total system throughput. A true high-speed multiuser wireless system can only be achieved through an increase in system spectral efficiency, measured in bits per second per Hertz per sector. The wireless multiple-input multiple-output (MIMO) communication systems seek to achieve capacities that are close to the Shannon limit by employing multiple transmit and receive antennas, as well as advanced space-time signal processing techniques.

In the past, receiver diversity has been used to mitigate the detrimental effects of multipath fading. Antenna elements at the receiver are spaced sufficiently far apart such that the signal received at each antenna can be viewed as having propagated through independent fading channels. Each path has a distinct and time-varying amplitude, phase and angle of arrival. The received signals are then combined using

optimal weights, forming a signal with better quality than each individual one. Three common diversity schemes are maximum ratio combining (MRC), equal gain combining (ECG) and selection combining (SC).

Recently, increasing research efforts have been focused on spatial diversity options for both the mobiles and basestation. With current 3G cellular systems using 2.4 GHz and 5 GHz carrier frequencies, mobiles will be able to carry multiple antennas with sufficient spacing without having to increase their size significantly. Various MIMO schemes are currently under consideration for 4G wireless communication systems. One of the most promising space-time processing techniques is the Bell Labs Layered Space-Time (BLAST) system proposed by Fochini [26]. In a rich scattering channel, the multiple antennas form, in effect, multiple single-input single-output (SISO) channels since each spatial multiplexed path fades independently from one another. The capacity of the BLAST architecture, therefore, increases linearly with the number of spatial multiplexed paths formed.

1.3 Wireless Communications Channel

Any communications system in the mobile radio channel suffers from a time-varying channel phenomenon known as multipath fading. The time-variant impulse response of the channel is a consequence of the constantly changing physical characteristics of the media.

The channel is said to be frequency-nonselective if the signal bandwidth is much smaller than the coherence bandwidth of the channel. Under such a scenario, the channel has constant gain and linear phase over the transmitted signal bandwidth. The received signal is therefore simply the transmitted signal multiplied by a

complex-valued, time-varying channel coefficient. Since all received multipath components undergo the same attenuation and phase shift, they are not resolvable. The channel gains can be modeled as complex Gaussian random variables with zero mean in a Rayleigh fading environment, where there is sufficient local scatterering. Ricean fading occurs when there exists a line-of-sight between the transmitter and receiver, and the channel gains can be modeled as complex Gaussian random variables with non-zero mean.

The transmitted signal is subjected to different channel gains and phase shifts across the frequency band if the signal bandwidth is larger than the coherence bandwidth of the channel. In such a case, the channel is said to be frequency-selective. In the time domain, frequency-selectivity occurs when the signalling period is smaller than the multipath delay spread of the channel. Multiple replicas of the transmitted signal, each with different amplitude and delay, arrive at the receiver and cause inter-symbol interference. In this case, the received multipath signals are resolvable, and the number of resolvable signal components is the product of the signal bandwidth and the multipath delay spread of the channel.

The rapidity of the fading is determined by the coherence time, which is a statistical measure of the time period over which the channel impulse response is essentially time-invariant. If the symbol duration is smaller than the coherence time of the channel, the channel attenuation and phase shift are essentially fixed for the duration of at least one signalling interval. When this condition holds, the channel is referred to as slow fading channel. Otherwise, the channel response changes rapidly during the symbol period, and is termed fast fading.

1.4 Motivation

Wireless MIMO systems have been traditionally studied in point-to-point communications, where exchange of information involve only a single pair of transmit and receive terminals. However, with space-time processing techniques being considered for use in 4G cellular wireless communication systems, researchers have begun exploring various multicast systems involving the MIMO paradigm [27]-[29]. By combining a CDMA system equipped with MUD that is near-far resistant with a spectrally-efficient MIMO system, the resulting multiuser CDMA MIMO (MCM) system offers potentially promising high-speed communications for 4G cellular wireless networks.

Current state-of-the-art MCM receivers utilize computationally-intensive processing techniques, such as BLAST, decorrelating, and pre-whitening. These MCM receivers also assume perfect estimation of channel state information (CSI). While ideal channel conditions and favourable assumptions lead to impressive performances, estimation errors result in non-ideal receiver performance. Timing mismatch, a source of performance degradation for CDMA systems, has not been thouroughly investigated in the BLAST research literature. Furthermore, in MCM wireless systems, and to the best of our knowledge, no research has been done on the impact of timing estimation errors for the time-delays between each transmit-receive antenna pair.

1.4 Thesis Contributions

The primary contributions of this thesis are briefly summarized as follows:

- This thesis investigates a more realistic model that takes into consideration

mismatch in time-delay estimation between transmit-receive antenna pairs. Time-delay mismatch will be shown to cause severe performance degradation to receivers that assume perfect timing.

- A novel space-time SIC that is robust to timing mismatch is proposed in this thesis. The robust space-time SIC (RSTSIC) receiver utilizes receiver diversity by combining the received signals from each antenna using optimum weights. In addition, amplitude averaging and soft-decision interference cancellation procedures are implemented to mitigate noise enhancement and error-propagation.
- The RSTSIC is shown to have performance very close to that of the space-time decorrelator with perfect time-delay information. Moreover, RSTSIC performance is shown to be insensitive to large time-delay estimation errors. Complexity is shown to be linear in the number of users, antennas and bits transmitted per frame.
- In the case of a MCM system under timing mismatch, independent fading and wide angle spread scattering, it is found that random codes are not suitable for spreading to combat multiple-access interference introduced by the multiple transmit antennas. It is found instead that the same Gold code may be effectively used to spread all data substreams of a user to maximize system capacity.

1.5 Thesis Outline

Chapter 2 of this thesis begins with an overview of multiuser detection. The discrete baseband model is introduced, followed by a brief introduction to the conventional

CDMA receiver and the optimum multiuser detector. Linear and multistage sub-optimum multiuser receivers are then described. The last subsections of this chapter explain the theory, transmission scheme and detection algorithms of a wireless MIMO communications system.

In Chapter 3, we present a MCM system model, where transmission scheme and channel assumptions are described. Next, a survey of the current state-of-the-art MCM receivers is presented, followed by the formulation of the proposed robust space-time SIC. The concept of soft-decision functions is discussed, and the generalized clipper decision function is then applied to the RSTSIC algorithm along with amplitude averaging. Finally, the BER and computation complexity of the RSTSIC are briefly analysed.

Having laid the groundwork in the previous chapters, we perform computer simulations in Chapter 4. We first investigate single-user MIMO receiver performance under a multiuser environment. The impact of timing error on the performance of existing MCM receivers are studied, and compared to the proposed RSTSIC. We then more thoroughly examine properties and performances of the RSTSIC under various conditions. The chapter ends with a discussion on spectrally-efficient transmission strategies.

Chapter 5 concludes this thesis and provides several suggestions for future work.

Chapter 2

Background

In this chapter, we review the basic attributes of MUD and MIMO systems. Various optimum and suboptimum multiuser receivers are first presented, as well as discussions of their advantages and disadvantages. In Section 2.2, a classic wireless MIMO communications model and its detection algorithms are described.

2.1 CDMA Multiuser Detection

In cellular CDMA systems, performance is limited by interference from co-channel users, or MAI. The advent of MUD in the late 1980s brought on a whole new horizon for cellular networks, as stringent power control became no longer necessary. However, new technological challenges arise even for today's real-time digital signal processors as the new receivers exhibit high computational complexity and latency. In this subsection, we introduce the important signal processing techniques used in the conventional and optimal receivers, as well as suboptimal receivers proposed subsequently that attempt to balance the trade off between complexity and performance.

2.1.1 Optimum Multiuser Detection

Consider an asynchronous CDMA system with K users sharing an additive white Gaussian noise (AWGN) multiple-access channel. Assuming a quasi-static channel, the amplitude and timing delay of each user can be considered as constants during the transmission in a frame of M bits, which are binary phase-shift keyed (BPSK) modulated. The received signal after down-conversion to baseband therefore is

$$r(t) = \sum_{k=1}^{K} \sum_{i=1}^{M} a_k b_k[i] S_k(t - iT_S - \tau_k) + n(t) \tag{2.1}$$

where

$$S_k(t - iT_S) = \sum_{l=0}^{L-1} c_k(l + iL)\, p(t - lT_C - iT_S) \quad S_k(t) \in [0, T_S) \tag{2.2}$$

$S_k(t)$ is the deterministic signature waveform for user *k*, normalized to have unit energy

$$\| S_k \|^2 = \int S_k^*(t) S_k(t) dt = 1 \tag{2.3}$$

$p(t)$ is a rectangular pulse of duration [0,Tc)

$c_k(l) \in \{-1,1\}$ is the PN code sequence assigned to the *k*th user

$L = \frac{T_S}{T_C}$ is the length of PN code sequence

T_S is the symbol interval

T_C is the chip interval

a_k is the received amplitude of the *k*th user's signal

$b_k[i] \in \{-1,1\}$ is the BPSK modulated *i*th raw data bit transmitted by the *k*th user

τ_k is the time delay of user *k*, where it is assumed that $0 \le \tau_k < T_S$

$n(t)$ is the white Gaussian noise with power spectral density σ^2

Throughout this thesis, $(\cdot)^*$, $(\cdot)^T$, and $(\cdot)^H$ denote the conjugate, transpose, and conjugate transpose operations, respectively.

Fig. 2.1 depicts a block diagram of a CDMA multiuser detector. The receiver front-end can be identical for both the conventional single-user detector and multiuser detectors and consists of a bank of matched filters, each matched to a particular user's PN sequence. The outputs of the bank of K matched filters are then sampled at the symbol rate, and can be expressed as

$$\begin{aligned} y_k(i) &= \int_{iT_S+\tau_k}^{(i+1)T_S+\tau_k} r(t)S_k(t-iT_S-\tau_k)dt \\ &= \int_{-\infty}^{\infty} \sum_{j=1}^{K} \sum_{m=1}^{M} a_j b_j[m] S_j(t-mT_S-\tau_j) S_k(t-iT_S-\tau_k)dt \\ &+ \int_{-\infty}^{\infty} n(t)S_k(t-iT_S-\tau_k)dt \\ &= \int_{-\infty}^{\infty} \sum_{m=1}^{M} a_k b_k[m] S_k(t-mT_S-\tau_k) S_k(t-iT_S-\tau_k)dt \\ &+ \int_{-\infty}^{\infty} \sum_{j\neq k,\, j=1}^{K} \sum_{m=1}^{M} a_j b_j[m] S_j(t-mT_S-\tau_j) S_k(t-iT_S-\tau_k)dt \\ &+ \int_{-\infty}^{\infty} n(t)S_k(t-iT_S-\tau_k)dt \\ &= a_k b_k[i] + \sum_{j\neq k,\, j=1}^{K} \sum_{m=1}^{M} \rho(jk,mi) + n(k,i) \end{aligned} \tag{2.4}$$

where the first term is the result of Equation (2.3),

$\rho(jk,mi) = \int_{-\infty}^{\infty} S_j(t-mT_S-\tau_j) S_k(t-iT_S-\tau_k)dt$, and

$n(k,i) = \int_{-\infty}^{\infty} n(t)S_k(t-iT_S-\tau_k)dt$. From Equation (2.4), we see that the matched filter output $y_k(i)$ is composed of three terms: the desired information $a_k b_k[i]$, the MAI $\rho(jk,mi)$ and the noise $n(k,i)$.

Collectively, the matched filter outputs for all K users and M symbols can be expressed in a long vector as

$$\mathbf{y} = [\mathbf{y}^T(1) \quad \ldots \quad \mathbf{y}^T(M)]^T \tag{2.5}$$

where

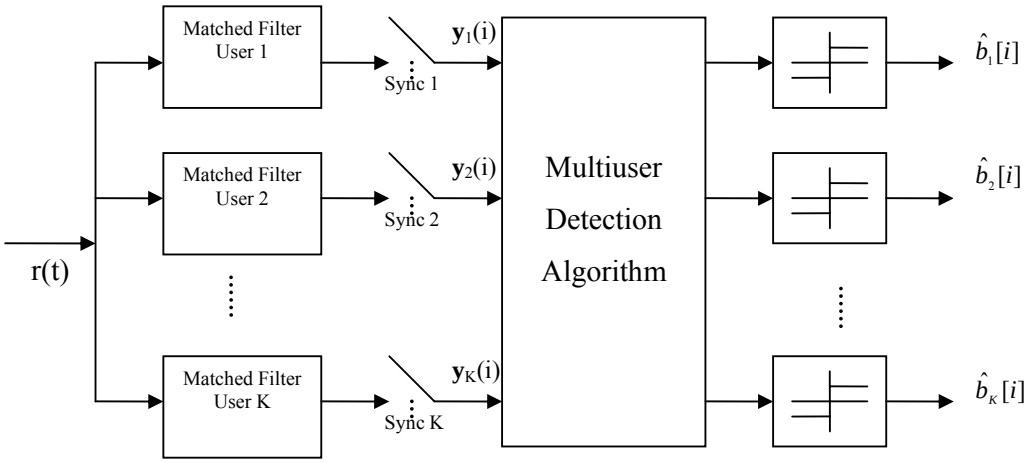

Figure 2.1. General block diagram of a CDMA multiuser receiver

$$\mathbf{y}(i) = [y_1(i), \quad \ldots, \quad y_K(i)]^T \tag{2.6}$$

is the matched filter output vector for K users in the *i*th symbol period.

The conventional single-user detector performs symbol estimation directly and independently on each of the $y_k(i)$ matched filter outputs, treating the MAI as white noise. Matched filtering relies solely on the signal constellation and PN code assignment to reduce MAI caused by PN sequence crosscorrelations. This detection method is optimum in the single-user case, or if all user PN code sequences are mutually orthogonal. The matched filter receiver works reasonably well in a multiuser environment if there are few users with low correlation sequences and the received powers from different users are nearly equal. However, in mobile wireless environments, the receiver suffers from deep fading and the near-far effect, where interfering users' powers are much greater than the desired user, which renders the conventional detector useless. In addition, orthogonality between the PN sequences can be destroyed by multipath signal propagation. Thus, using a conventional

receiver, MAI is severe and the performance is very poor for uncoded wireless systems.

Until the mid 1980's, the matched filter was regarded as the optimum CDMA receiver, and system limitations such as the near-far effect were regarded as an inherent limitation of the CDMA system. In 1986, Verdú proved that the near-far problem is not an inherent limitation of CDMA itself, but of the matched filter receiver [3]. Verdú formulated a multiuser receiver based on the maximum-likelihood (ML) criteria, which is equivalent to the optimum maximum a priori (MAP) criteria when the transmitted sequences are equiprobable. The proposed receiver consists of a front-end matched filter bank, followed by a Viterbi forward dynamic programming detection algorithm that selects the sequence **b** that maximizes the conditional probability $P\left[\{r(t), t \in \Re\} \mid \mathbf{b}\right]$. The matched filter output vector **y** provides sufficient statistics for optimum detection. In [3], an optimum minimum-probability-of-error detector is also proposed using the same front-end matched filter bank, followed by a backward-forward dynamic programming detection algorithm. These receivers attain essentially single-user performance with the assumption that timing, amplitude and signature waveforms of all the active users are all known. Although the optimum detectors significantly outperform the conventional detector, they do so at the expense of increased complexity that is exponential in the number of users in the system.

2.1.2 Linear MUD

The disparity in complexity and performance between the conventional detector and optimum multiuser detectors motivated researchers to seek suboptimum alternatives that exhibit better performance/complexity tradeoffs. A group of linear multiuser detectors that are generalizations of single-user intersymbol interference (ISI) channel

equalizer counterparts are formulated in [4] and [5]. As seen in Fig. 2.1, linear multiuser detectors perform linear transformations on the matched filter output **y**, which can be expressed as

$$\mathbf{y} = \mathbf{RAb} + \mathbf{n} \tag{2.7}$$

where the zero-mean Gaussian noise vector **n** has the MKxMK covariance matrix $\sigma^2\mathbf{R}$,

$$\mathbf{R} = \begin{pmatrix} \mathbf{R}(0) & \mathbf{R}(-1) & 0 & \cdots & 0 \\ \mathbf{R}(1) & \mathbf{R}(0) & \mathbf{R}(-1) & & \vdots \\ 0 & \mathbf{R}(1) & \mathbf{R}(0) & \ddots & 0 \\ \vdots & & \ddots & \ddots & \mathbf{R}(-1) \\ 0 & \cdots & 0 & \mathbf{R}(1) & \mathbf{R}(0) \end{pmatrix} \tag{2.8}$$

$$\mathbf{A} = diag\{a_1(1),...,a_K(1),...,a_1(M),...,a_K(M)\} \tag{2.9}$$

$$\mathbf{b} = [\mathrm{b}_1(1),\ldots,\mathrm{b}_\mathrm{K}(1),\ldots,\mathrm{b}_1(\mathrm{M}),\ldots,\mathrm{b}_\mathrm{K}(\mathrm{M})]^\mathrm{T} \tag{2.10}$$

The (k, j) th element of the KxK signal correlation matrix **R**(m) is:

$$\mathbf{R}_{k,j}(m) = \int_{-\infty}^{\infty} S_k(t-\tau_k)S_j(t+mT_S-\tau_j)dt \tag{2.11}$$

and $\mathbf{R}(m)$ has the following properties

$$\begin{aligned} \mathbf{R}(m) &= 0, \quad \forall \mid m \mid > 1 \\ \mathbf{R}(-m) &= \mathbf{R}^T(m) \end{aligned}$$

Let **w** be a linear transformation vector for the multiuser detector. The decision vector is

$$\mathbf{d} = \mathbf{w}^T\mathbf{y} \tag{2.12}$$

The decorrelating detector in [4] has a linear transformation equivalent to the inverse of the correlation matrix

$$\mathbf{w} = \mathbf{R}^{-1} \tag{2.13}$$

The decision vector is then

$$\mathbf{d} = \mathbf{R}^{-1}(\mathbf{RAb} + \mathbf{n}) = \mathbf{Ab} + \mathbf{R}^{-1}\mathbf{n} \tag{2.14}$$

and since BPSK is used, the bit decision is determined by the sign of the decision vector

$$\hat{\mathbf{b}} = sign(\mathbf{d}) \tag{2.15}$$

The decorrelator can be viewed as a modified matched filter orthogonal to the MAI, and similar to the zero-forcing (ZF) equalizer. This receiver has quadratic complexity in the number of users, and is optimum in three senses: near-far resistant, leastsquares, and ML when the received amplitudes are unknown [4]. A multiuser detector is said to be near-far resistant if its asymptotic multiuser efficiency is non-zero over all possible received energies of all other users, where asymptotic multiuser efficiency quantifies the performance loss due to the existence of other users in the channel [44]. The decorrelator receiver has the advantage that knowledge of the received amplitudes is not required. However, the inversion of the channel performed by the decorrelator enhances the background noise, given by the noise vector $\mathbf{R}^{-1}\mathbf{n}$ in equation (2.14).

The decision vector has covariance matrix

$$E[(\mathbf{R}^{-1}\mathbf{n})(\mathbf{R}^{-1}\mathbf{n})^{H}] = \sigma^{2}\mathbf{R}^{-1} \tag{2.16}$$

which can results in noise power enhancement, creating a gap between the single-user error performance and the decorrelator error probability.

Another linear detector with the same structure is proposed in [5] based on the optimization of the minimum mean-squared error (MMSE) criteria:

$$\mathbf{w} = \min_{w} E[(\mathbf{b} - \hat{\mathbf{b}})^{T}(\mathbf{b} - \hat{\mathbf{b}})] \tag{2.17}$$

The solution to the above equation is

$$\mathbf{w} = (\mathbf{R} + \sigma^{2}(\mathbf{A}^{T}\mathbf{A})^{-1})^{-1} \tag{2.18}$$

While the single-user matched filter combats white noise exclusively and the decorrelator eliminates MAI disregarding background noise, the MMSE linear detector forms a compromise between the two, taking the relevant importance of the background noise and interfering users into account. In fact, the decorrelator and conventional detectors are limiting cases of the MMSE linear detector: the MMSE detector performance approaches that of the conventional detector as the background noise variance goes to infinity, and that of the decorrelator as the background noise variance goes to zero. Therefore, the MMSE linear detector also achieves the same optimum near-far resistance as that of the decorrelator.

2.1.3 Multistage Decision-Driven MUD

A number of different non-linear multiuser detection strategies in multiuser detection have been proposed based on multistage and decision feedback processing. One simple and natural idea, the multistage SIC, was proposed in [6]. In SIC, the strongest user is detected first using a conventional matched-filter, ignoring all other users with smaller energies; this requires the detector to order the users according to signal strength. Assuming hard decisions are employed, the *j*th stage bit estimate of the *k*th user is

$$\hat{b}_k^j(m) = sign[y_k^j(m)] \tag{2.19}$$

where

$$y_k^j(m) = y_k^0(m) - \sum_{l=k+1}^{K} \mathbf{R}_{k,l}(1)\hat{b}_l^j(m-1) - \sum_{l\neq k} \mathbf{R}_{k,l}(0)\hat{b}_l^j(m) - \sum_{l=1}^{k-1} \mathbf{R}_{k,l}(-1)\hat{b}_l^{j+1}(m+1) \tag{2.20}$$

and the initial bit estimate can be obtained by the conventional matched filter output

$$\hat{b}_k^1(m) = sign[y_k^0(m)] \tag{2.21}$$

The SIC receiver reconstructs the signal using the bit estimate (2.19) and subtracts it from the composite received signal. This will cancel the interfering signal provided that the decision was correct, and that the receiver has accurate amplitude and timing information. The initial bit and output estimates of the detector can be improved by using other suboptimum schemes, such as a decorrelating first stage, depending on the complexity one is able to tolerate.

The SIC has the advantage that its complexity is linear in the number of active users, and very little computation is required relative to the linear detectors. Despite its simple structure, a shortcoming of the SIC is that any errors in amplitude estimation and intermediate decisions will translate directly into noise or MAI for future decisions. This problem can be mitigated by using soft intermediate decisions or weighted signal cancellation according to each user's power level: strong users are much more reliable, and are subtracted with more weight, while only small proportions of weak users' signals are stripped away. When a linear decision function is employed, the linear SIC is shown to correspond to applying Gauss-Seidel iteration to approximate matrix inversion [32], and thus power-ordering is not required.

A single-stage decision-feedback detector is studied in [30]. The detector, shown in Fig. 2.2, consists of a feed-forward filter fed by matched filter outputs and a feedback filter fed by past decisions. Under the white noise model, the optimum decorrelating decision-feedback detector tries to maximize the SNR at the decision device, and the filters are obtained through spectral factorization. The discrete model in Equation (2.7) can be represented in the z-transform domain as

$$\mathbf{y}(z) = \mathbf{S}(z)\mathbf{A}\mathbf{b} + \mathbf{n}(z) \tag{2.22}$$

where

$$\mathbf{S}(z) = \mathbf{R}^T(1)z + \mathbf{R}(0) + \mathbf{R}(1)z^{-1} \tag{2.23}$$

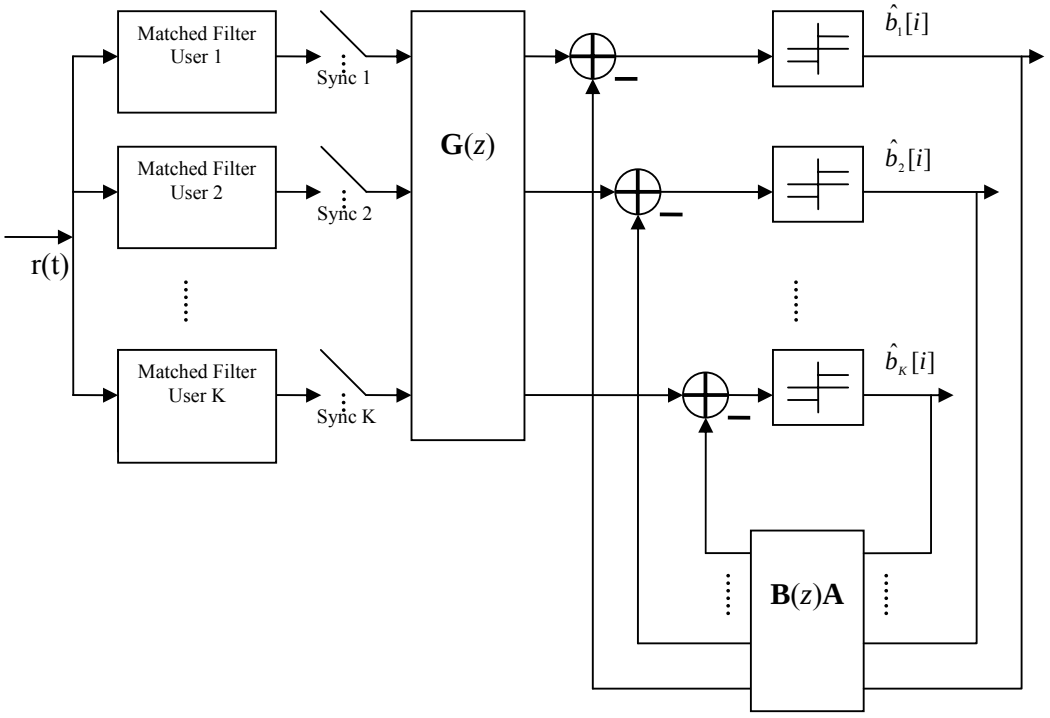

Figure 2.2. Multistage decision-feedback multiuser receiver

$$\mathbf{n}(z) = (\mathbf{F}^T(0) + \mathbf{F}^T(1)z)\overline{\mathbf{n}} \tag{2.24}$$

$\overline{\mathbf{n}}$ is independent Gaussian with covariance $\sigma^2\mathbf{I}$, $\mathbf{R}$(m) is defined in Equation (2.11), and can be factored as

$$\mathbf{R}(0) = \mathbf{F}^T(0)\mathbf{F}(0) + \mathbf{F}^T(1)\mathbf{F}(1) \tag{2.25}$$

$$\mathbf{R}(1) = \mathbf{F}^T(0)\mathbf{F}(1) \tag{2.26}$$

where $\mathbf{F}(0)$ is lower triangular and $\mathbf{F}(1)$ is upper triangular with zero diagonal. From (2.25) and (2.26), the matrix $\mathbf{S}(z)$ can represented by

$$\mathbf{S}(z) = [\mathbf{F}(0) + \mathbf{F}(1)z]^T[\mathbf{F}(0) + \mathbf{F}(1)z^{-1}] \tag{2.27}$$

The bit estimate of the asynchronous decorrelating decision-feedback receiver is shown to be

$$\hat{\mathbf{b}} = sign[\mathbf{G}(z)\mathbf{y}(z) - \mathbf{B}(z)\mathbf{A}\hat{\mathbf{b}}] \tag{2.28}$$

where

$$\mathbf{G}(z) = [\mathbf{F}(0) + \mathbf{F}(1)z]^{-T} \tag{2.29}$$

$$\mathbf{B}(z) = \mathbf{F}(0) - diag\mathbf{F}(0) + \mathbf{F}(1)z^{-1} \tag{2.30}$$

The optimal feed-forward filter **G**(*z*) is derived to be the noise whitening filter that cancels MAI for those bits that have not yet been detected, while the feedback filter **B**(*z*) attempts to eliminate MAI by regenerating and cancelling the interfering signals from the detected bits. The feedback filter can take advantage of its causal structure by demodulating users in the order of decreasing energy, so that the decisions made for the stronger users can be utilized by the weaker users.

The decision-feedback detector is inherently more complex than other decision-driven counterparts, due to the need for performing a spectral decomposition in obtaining the filter coefficients. However, the filter coefficients can be adaptively updated for each symbol interval, and a MMSE decision-feedback detector is proposed in [31] by the same author.

2.2 Multiple Input Multiple Output Communication Systems

In order to support high-speed Internet applications while ensuring the quality of service (QoS), the spectral efficiencies of the next generation of wireless networks has to be greatly enhanced. The concept of multiple-input multiple-output (MIMO) systems introduced in the mid 1990s demonstrated that using multiple antenna elements at both the receiver and the transmitter can result in enormous capacity gains [26], [46]. Since then, various MIMO architectures have been proposed such as space-time block coding [34], [47] and smart antenna beamforming [48]. In this

chapter, we shall focus on an early and well-known high-rate MIMO architecture, known as the Bell Labs Layered Space-Time system.

2.2.1 Bell Labs Layered Space-Time Architecture

The BLAST is a narrowband point-to-point communication architecture for achieving high spectral efficiency. The diagonally-layered space-time architecture, now known as diagonal BLAST or D-BLAST, is proposed by Foschini [26]. It uses multiple antennas at both the transmitter and receiver, and a codec architecture that disperses the coded blocks across the diagonals in space-time. In a rich Rayleigh scattering environment, this codec structure has capacity that increases linearly with the number of antenna elements, up to 90% of the Shannon theoretical capacity limit. However, D-BLAST suffers from high implementation complexity, and a simplified coding technique, vertical BLAST or V-BLAST, is proposed in [33]. The essential difference between D-BLAST and V-BLAST lies in their respective transmission coding processes. In D-BLAST, temporal redundancy is introduced between the substreams by dispersing the code blocks along the space-time diagonals. In V-BLAST, however, the encoding process is simply a demultiplexing operation. The inter-substream block coding technique is what leads to D-BLAST's higher spectral efficiency. For a large number of antennas, D-BLAST can offer at most 30% increase in capacity over V-BLAST. The receiver processing for V-BLAST is much simplified over D-BLAST, however, since the nulling and cancellation detection algorithm does not extend across the temporal domain.

A high-level block diagram of a V-BLAST system is shown in Fig. 2.3. Consider a point-to-point system where the number of transmit antennas is N_T and the number of receive antennas is N_R. A single bit stream is demultiplexed into several

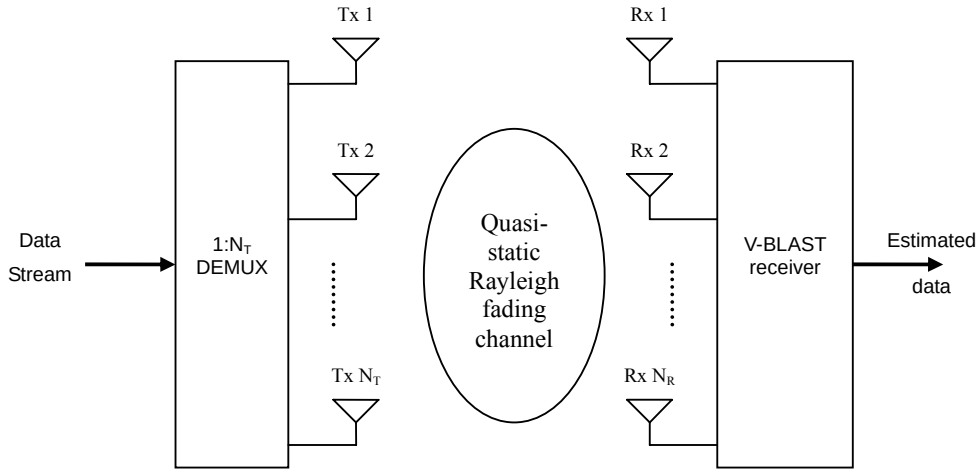

Figure 2.3. System block diagram of a MIMO V-BLAST system

substreams, and each substream is then modulated independently and sent through a separate transmit antenna. If we assume ideal Rayleigh propagation, the channel between each transmit and receive antenna pair can be characterized by a complex Gaussian amplitude coefficient. Therefore, the signal received from each substream can be represented by a complex vector with dimension N_R modulated by its data symbol, and the total received signal is the sum of the signals received from each of the N_T substreams and Gaussian noise. Note that we can think of the complex N_R-vector for each substream as a complex spatial-spreading code. Moreover, if N_R is equal or greater than N_T, and there is rich scattering in the channel such that the substream channel vectors are independent, one can use the V-BLAST detection algorithm to demodulate the substream based only on the spatial characteristics formed by the antenna array.

2.2.2 System Model

At the transmitter, a single data stream is demultiplexed into N_T substreams, and each substream is then encoded independently into symbols and fed to its respective transmitter. Transmitters 1:N_T are themselves ordinary BPSK transmitters, and they operate co-channel at symbol rate $1/T_S$ symbols/sec, with synchronized symbol timing.

The wireless channel is assumed to be quasi-static, flat fading, and rich scattering. The complex fading coefficients between each antenna pair are assumed to be independent, and have been estimated at the receiver by a short training sequence prior to the detection procedure.

In the following, we take a discrete-time, complex baseband view of the system model for a single transmitted vector symbol, assuming symbol-synchronous receiver sampling and perfect timing estimation. After matched filtering and symbol rate sampling, we can represent the received signals at the N_R receive antennas as:

$$\mathbf{r} = [r_1, \quad r_2, \quad \ldots \quad r_{N_T}]^T \tag{2.31}$$

The transmitted vector symbols from N_T transmit antennas can also be organized into vector form:

$$\mathbf{b} = [b_1, \quad b_2, \quad \ldots \quad b_{N_T}]^T \tag{2.32}$$

Therefore, the received signal can be expressed as a linear combination of the transmitted signal **b**:

$$\mathbf{r} = \mathbf{C}\mathbf{b} + \mathbf{n} \tag{2.33}$$

where **C** is the N_R-by-N_T complex channel matrix, and **n** is the complex AWGN with spatially and temporally white components of identical power σ^2 at each of the N_R receivers.

Due to an assumed rich-scattering environment, the elements of the matrix **C** are

outcomes of independently and identically distributed (i.i.d.) complex Gaussian variables of unit variance. The channel matrix can be partitioned into columns corresponding to the N_T transmitted signals:

$$\mathbf{C} = [\mathbf{c}_1, \quad \mathbf{c}_2, \quad \ldots \quad \mathbf{c}_{N_T}]^T \tag{2.34}$$

2.2.3 V-BLAST Detection Algorithm

Here we describe the technique for symbol detection in V-BLAST first proposed in [33]. Taking advantage of the inherent timing synchronism in the system model, ordered SIC is used along with linear nulling to perform symbol detections. The criterion of SIC ordering in the V-BLAST algorithm is based on the maximization of post-detection signal-to-interference plus noise ratio (SINR). It is shown that this method of ordering is indeed globally optimal. The ZF criterion is chosen for the nulling process to simplify the algorithm description, although the MMSE criterion can be applied in a similar process.

Let j index the iteration, where $1 \leq j \leq N_T$

Step (1): Calculate the inverse of the correlation matrix formed from the channel:

$$\mathbf{R}(j)^{-1} = \mathrm{Re}[\mathbf{C}^H(j)\mathbf{C}(j)]^{-1}$$

Step (2): Find the substream, g, whose post-decorrelator SNR is the highest, corresponding to the minimum among the first N_T-j+1 diagonal entries of $\mathbf{R}(j)^{-1}$:

$$g = \arg\min[\mathbf{R}^{-1}(j)_{(g,g)}], \quad g = 1,\ldots, N_T - j + 1$$

The nulling vector $\mathbf{w}$ is the gth row of $\mathbf{R}(j)^{-1}$, and the bit estimate of the gth substream is:

$$\hat{\mathbf{b}}(j) = sign(\mathbf{w}\mathbf{r}(j))$$

Step (3): Perform interference cancellation by subtracting the detected signal from the received signal:

$$\mathbf{r}(j+1) = \mathbf{r}(j) - \mathbf{c}_g \hat{\mathbf{b}}(j)$$

Reorder $\mathbf{C}(j)$ such that the gth column and the last column are interchanged:

$$\mathbf{C}(j)' = [\mathbf{c}_1 \quad \ldots \quad \mathbf{c}_j \quad \ldots \quad \mathbf{c}_{N_T} \quad \mathbf{c}_g] = [\mathbf{C}(j+1)\mathbf{c}_g]$$

where $\mathbf{C}(j+1)$ is defined as $\mathbf{C}(j)'$ with the last column $\mathbf{c}_g$ deleted.

Step (4): Go back to Step 1, increment j and repeat until all N_T substreams have been detected.

The V-BLAST capacity has been shown to grow linearly with the number of antennas. For large SNR, if an optimum number of N_{opt} transmit antennas are used, then for each 3 dB coding gain, the benefit is roughly an additional N_{opt} bits/s/Hz. Impairments such as timing error, phase noise, carrier frequency offset and imperfect channel estimate can cause significant system performance degradation. Furthermore, non-ideal channel conditions such as multipath, fast fading and correlation will also have large, negative impact on performance of the system.

Chapter 3

Multiuser CDMA MIMO Systems

The ever-increasing demand on wireless communications today has led to a tremendous need a greater spectral-efficiency. Therefore, a significant focus of late has been to develop systems that offer both high capacity, such as that of V-BLAST, along with MAI resistance, especially in the downlink (from basestation to mobile). Given the enormous potential of multiuser CDMA MIMO (MCM) systems, researchers have recently begun to investigate the possible capacity and bit error rate (BER) performance of such systems [27]-[29]. In this chapter, we present a downlink model of the MCM system, followed by an overview of current state-of-the-art MCM receivers. We will then propose several robust MCM receivers, leading to the formulation of the robust space-time SIC (RSTSIC). Amplitude averaging and the generalized clipper decision function are then incorporated into the RSTSIC. Finally, performance and complexity are analyzed.

3.1 System Description

We consider the downlink receiver that has knowledge of the signature waveforms for all users. While a similar model appears in [27], there have been few treatments of

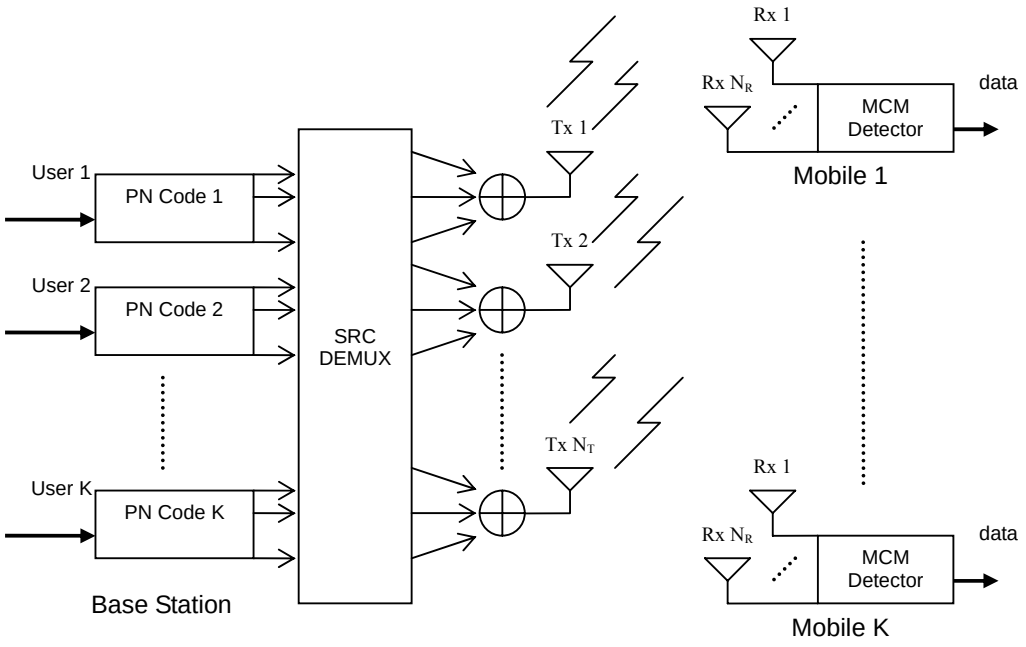

Figure 3.1. System block diagram of a multiuser CDMA MIMO system

MCM systems in the literature. To date, the issue of timing error effects have not been addressed. The system consists of K users, each equipped with N_R receive antennas to demodulate N_T independent data substreams transmitted from a single basestation with N_T antennas. Figure 3.1 shows the general block diagram of the proposed system. The KN_T data substreams are each spread by a length L spreading code and then transmitted through a rich-scattering channel. Antennas are assumed to be far enough apart such that the complex fading coefficients among the antennas are uncorrelated. It is assumed that time delays between antenna pairs are independent, and are restricted to lay within one symbol interval. To focus on timing errors, edge effects [37] are eliminated by using an isolation bit insertion receiver [38]. By inserting a blank bit interval after every M bit intervals and selecting the received signal of length M+1 symbols, the interference from the next frame is effectively

blocked from the current one. For clarity and brevity, we consider only single-path channels. However, the model and methods presented here can be extended to the case of multipath channels in a straight-forward manner. The coherently received complex baseband signal for a frame of M data bits at the *p*th (p=1, ..., N_R) antenna is

$$r_p(t) = \sum_{m=1}^{M} \sum_{n=1}^{N_T} \sum_{k=1}^{K} c_{n,p} a_{k,n} s_k(t - mT_s - \tau_{n,p}) b_{k,n}(m) + n_p(t) \tag{3.1}$$

where $c_{n,p}$ is the complex channel coefficient between the *n*th transmit antenna and the *p*th receive antenna, $a_{k,n}$ is the amplitude of the *k*th user's *n*th substream, $s_k(t)$ is the normalized PN code sequence of the *k*th user, T_s is the symbol interval, $\tau_{n,p}$ is the time delay of the path between the *n*th transmit antenna and the *p*th receive antenna, $b_{k,n}(m)$ is the BPSK modulated data symbol of the *k*th user's *n*th substream, and $n_p(t)$ is the AWGN on receive antenna *p*. The channel amplitudes are independent, zero-mean complex Gaussian variables with unit variance

$$E(c^*_{n1,p1} c_{n2,p2}) = \mathbf{I}_{N_T N_R} \tag{3.2}$$

where $\mathbf{I}_N$ denotes an identity matrix of size N, $(\cdot)^*$ denotes the complex conjugate.

After chip matched filtering and chip rate sampling, the discrete-time complex baseband received signal from (3.1) at its *p*th antenna for a frame of M data bits can be written as a complex (M+1)L-vector

$$\mathbf{r}_p = \mathbf{S}_p \widetilde{\mathbf{C}}_p \mathbf{A}\mathbf{b} + \mathbf{n}_p \tag{3.3}$$

where

$$\mathbf{S}_p = [\mathbf{S}_{k,n,p}(1) \quad \mathbf{S}_{k,n,p}(2) \quad \cdots \quad \mathbf{S}_{k,n,p}(M)] \tag{3.4}$$

is the real (M+1)L-by-KMN_T spreading code matrix formed from concatenating the matrices

$$\mathbf{S}_{k,n,p}(i) = [\mathbf{s}_{1,1,p}(i) \quad \cdots \quad \mathbf{s}_{1,N_T,p}(i) \quad \mathbf{s}_{2,1,p}(i) \quad \cdots \quad \mathbf{s}_{K,N_T,p}(i)] \in \Re^{(M+1)L \times KN_T},$$

where each matrix consists of the columns

$$\mathbf{s}_{k,n,p}(i) = s_k(t - iL - \tau_{n,p}) \in \Re^{(M+1)L}$$

of spreading code vectors for the *k*th user's transmission over the *n*th antenna. Matrix $\widetilde{\mathbf{C}}_p$ is block diagonal of size KMN_T-by-KMN_T defined by KM instances of the channel matrix $\mathbf{C}_p$ along the main diagonal:

$$\widetilde{\mathbf{C}}_p = \mathbf{I}_{KM} \otimes diag\left(\underbrace{\mathbf{C}_p \quad \cdots \quad \mathbf{C}_p}_{N_T} \right) \tag{3.5}$$

where $\otimes$ denotes the Kronecker product. The matrix $\mathbf{C}_p$ is the complex N_T-by-N_T channel matrix defined by

$$\mathbf{C}_p = diag\begin{pmatrix} c_{1,p} & c_{2,p} & \cdots & c_{N_T,p} \end{pmatrix} \tag{3.6}$$

where $c_{n,p}$ is the complex coefficient corresponding to the fading channel between transmit antenna *n* and the receive antenna *p*. Matrix $\mathbf{A}$ is a KMN_T-by-MKN_T diagonal matrix of amplitudes defined by

$$\mathbf{A} = \mathbf{I}_M \otimes \mathbf{a} \tag{3.7}$$

where $\mathbf{a} = diag\begin{pmatrix} a_{1,1} & \cdots & a_{1,N_T} & a_{2,1} & \cdots & a_{K,1} & \cdots & a_{K,N_T} \end{pmatrix}$.

Vector $\mathbf{b}$ is the real KMN_T binary data vector defined by

$$\mathbf{b} = [\mathbf{b}_{k,n}^T(1) \quad \mathbf{b}_{k,n}^T(2) \quad \cdots \quad \mathbf{b}_{k,n}^T(M)]^T \tag{3.8}$$

and $\mathbf{b}_{k,n}(i) = [b_{1,1}(i) \quad \cdots \quad b_{1,N_T}(i) \quad b_{2,1}(i) \quad \cdots \quad b_{K,1}(i) \quad \cdots \quad b_{K,N_T}(i)]^T$ where BPSK is again assumed. Vector $\mathbf{n}_p$ is the zero-mean complex (circular symmetric) Gaussian noise (M+1)L-vector with independently and identically distributed (i.i.d.) components whose real and imaginary components each have variance $\frac{1}{2}\sigma^2$.

Note that all the substreams corresponding to a particular user have equal transmission energy, weighted by $\frac{1}{\sqrt{N_T}}$ in order to restrict the total power output for the users. The channel is assumed to be quasi-static; therefore $\widetilde{\mathbf{C}}_p \ \left(p = 1,\ldots,N_R\right)$ is fixed over the duration of the frame, and assumed to be perfectly estimated at the receiver. Also, since the composite signal multiplex goes through the same channel, fading coefficients and time delays between antenna pairs for all user signals are identical.

3.2 Multiuser CDMA MIMO Detectors

We will review a few state-of-the-art MCM receivers in this section. The performances of these receivers versus their single-user counterparts will be compared through simulation in the next chapter.

3.2.1 Space-Time Decorrelator with V-BLAST

In [27], transmission strategies, detection techniques and capacity are analyzed for the downlink of a multiple antenna cellular CDMA system. The received signal vector (3.3) at each branch is passed through a space-time matched filter [35], or two-dimensional (2-D) rake receiver, and combined to form the sufficient statistic vector **y** expressed as

$$\begin{aligned}\mathbf{y} &= \mathrm{Re}\left[\sum_{p=1}^{N_R} \widetilde{\mathbf{C}}_p^H \mathbf{S}_p^T \mathbf{r}_p\right] \\ &= \sum_{p=1}^{N_R} \mathrm{Re}\left[\widetilde{\mathbf{C}}_p^H \mathbf{S}_p^T \mathbf{S}_p \widetilde{\mathbf{C}}_p\right]\mathbf{A}\mathbf{b} + \sum_{p=1}^{N_R} \mathrm{Re}\left[\widetilde{\mathbf{C}}_p^H \mathbf{S}_p^T \mathbf{n}_p\right] \\ &= \mathbf{R}\mathbf{A}\mathbf{b} + \mathbf{n}\end{aligned} \tag{3.9}$$

where

$$\mathbf{R} = \sum_{p=1}^{N_R} \mathrm{Re}\left[\widetilde{\mathbf{C}}_p^H \mathbf{S}_p^T \mathbf{S}_p \widetilde{\mathbf{C}}_p\right] \tag{3.10}$$

A full space-time decorrelation is performed, followed by a combiner that re-introduces the correlation for the desired N_T substreams to form

$$\mathbf{h} = \left[(\mathbf{R}^{-1})_{[1:MN_T,1:MN_T]}\right]^{-1}\left[\mathbf{R}^{-1}\mathbf{y}\right]_{[1:MN_T]} \tag{3.11}$$

where $(\mathbf{R}^{-1}\mathbf{y})_{[1:MN_T]}$ denotes a vector with the first MN_T elements of the vector ($\mathbf{R}^{-1}\mathbf{y}$), and $(\mathbf{R}^{-1})_{[1:MN_T,1:MN_T]}$ denotes the upper-left MN_T-by-MN_T submatrix of $\mathbf{R}^{-1}$. Note that a space-time decorrelator (STD) simply takes the sign of the soft data estimates from the vector ($\mathbf{R}^{-1}\mathbf{y}$).

From the 1-by-MN_T vector $\mathbf{h}$, the desired N_T substreams in M frames are separated and estimated using the V-BLAST algorithm. We refer to this MCM receiver as the STD+VBLAST receiver.

3.2.2 Hybrid Linear Iterative MUD

A similar approach to that of the STD+VBLAST receiver is proposed in [28], named as the hybrid linear-iterative multiuser detector (HLIMUD). This receiver first obtains the soft bit estimation by cancelling MAI and self-interference using the MMSE criteria. It then reintroduces pre-whitened spatial correlation for decision-feedback cancellation.

The soft symbol estimates can be obtained after the space-time MMSE detector

$$\widetilde{\mathbf{b}} = \left[\sum_{p=1}^{N_R} \mathbf{X}_p^H \mathbf{X}_p + \sigma^2 (\mathbf{A}^T \mathbf{A})^{-1}\right]^{-1}\left[\sum_{p=1}^{N_R} \mathbf{X}_p^H \mathbf{r}\right] \tag{3.12}$$

where $\mathbf{X}_p = \mathbf{S}_p \widetilde{\mathbf{C}}_p$. The combiner, similar to the feed-forward filter in Eq. (2.27) is

$$\mathbf{G} = \mathbf{w}^{-\frac{1}{2}H} \tag{3.13}$$

where weight vector **w** is defined as

$$\mathbf{w} = \left[\sum_{p=1}^{N_R} \mathbf{C}_p^H \mathbf{C}_p + \sigma^2 (\mathbf{A}^T \mathbf{A})^{-1} \right]^{-1} \tag{3.14}$$

Therefore, we can obtain the bit estimate sequentially by

$$\hat{\mathbf{b}} = sign(\mathbf{G}\tilde{\mathbf{b}} - (\mathbf{G}^H - diag\{\mathbf{G}^H\}\hat{\mathbf{b}}) \tag{3.15}$$

3.2.3 Layered Space-Time MUD

Subsequently, a layered space-time multiuser detector (LAST-MUD) is proposed in [29] for the uplink. A number of mobiles, each equipped with one antenna, are grouped together and assigned one spreading code. Together, several of these groups form a pseudo-MCM system. The received vector at the basestation is again passed through the space-time matched filter, and then each of the substreams is ordered according to their respective SNRs. This implies that two successive decoded substreams do not have to belong to the same user, or even the same user group. The V-BLAST algorithm (Section 2.2.3) is then performed using the space-time correlation matrix, **R** in Equation (3.10), to obtain the data bit estimates.

A SIC LAST-MUD receiver based on the group detection concept [36] is also proposed in [29]. The serial layered space-time group multiuser detector (LASTG-MUD) successively obtains data estimates in groups of users that are assigned to the same spreading code, in the order of decreasing average SNRs. The detected set of data will then be removed from the sufficient statistic vector of the remaining groups. The process is repeated until all data are extracted.

The reduced complexity LASTG-MUD comes at the expense of higher BER.

Under the same system parameters, the serial LASTG-MUD requires higher bandwidth to achieve performance comparable to that of the LAST-MUD. Therefore, a trade-off has to be made between the quality of service (QoS) and system complexity.

All of the above-mentioned MCM receivers assume perfect knowledge of the channel state information (CSI). In practice, however, estimation errors are inevitable, leading to sub-ideal and sometimes very poor performances attained by these receivers.

3.3 MCM Detectors that are Robust to Delay Mismatch

3.3.1 Prediction Error Approach

Let the true time delay from the *n*th transmit antenna to the *p*th receive antenna be $\tau_{n,p} = (\rho_{n,p} + \delta_{n,p})T_C$, where T_C is the chip interval, $\rho_{n,p} \in \{0,1,\ldots,L-1\}$ is the integer part of the delay and $\delta_{n,p} \in [0,1)$ is the fractional part. Then $\mathbf{s}_{k,n,p}(i)$ can be expressed as a combination of two adjacent shifted versions of user spreading codes [38]

$$\mathbf{s}_{k,n,p}(i) = \delta_{n,p}\mathbf{d}_k(\rho_{n,p}+1,i) + (1-\delta_{n,p})\mathbf{d}_k(\rho_{n,p},i) \tag{3.16}$$

where $\mathbf{d}_k \in \Re^{(M+1)L}$ is the *k*th user's spreading code vector for the $(M+1)T_S$ second interval, defined as

$$\mathbf{d}_k = \left[\mathbf{d}_k(0) \quad \mathbf{d}_k(1) \quad \cdots \quad \mathbf{d}_k(L-1) \quad \underbrace{00\ldots0}_{ML}\right]^T \tag{3.17}$$

In (3.17), $\mathbf{d}_k(\rho_{n,p}, i)$ is defined as $\mathbf{d}_k$ right shifted by $(i-1)L + \rho_{n,p}$ chips. Assuming the receivers are under course timing acquisition such that the true time delays are estimated accurately within one chip interval, the prediction error approach in [25] can be applied. We can express the *k*th user's signature waveform for the *i*th interval, $\mathbf{s}_{k,n,p}(i)$, as the weighted sum of two signals, as shown in Fig. 3.2.

$$\begin{aligned}\mathbf{s}_{k,n,p}(i) &= \delta_{n,p}\mathbf{d}_k(\rho_{n,p}+1, i) + (1-\delta_{n,p})\mathbf{d}_k(\rho_{n,p}, i) \\ &= \left[\hat{\delta}_{n,p}\mathbf{d}_k(\rho_{n,p}+1, i) + (1-\hat{\delta}_{n,p})\mathbf{d}_k(\rho_{n,p}, i)\right] \\ &\quad + (\delta_{n,p}-\hat{\delta}_{n,p})\left[\mathbf{d}_k(\rho_{n,p}+1, i) - \mathbf{d}_k(\rho_{n,p}, i)\right] \\ &= \hat{\mathbf{s}}_{k,n,p}(i) + (\delta_{n,p}-\hat{\delta}_{n,p})\Delta\mathbf{s}_{k,n,p}(i)\end{aligned} \tag{3.18}$$

where $\hat{\tau}_{n,p} = (\rho_{n,p} + \hat{\delta}_{n,p})T_c$ is the estimated time delay from the *n*th transmit antenna to the *p*th receive antenna. From (3.18), we can view each user as the combination of two virtual users, one with estimated code vector $\hat{\mathbf{s}}_{k,n,p}(i)$, and the other with error code vector $\Delta\hat{\mathbf{s}}_{k,n,p}(i)$.

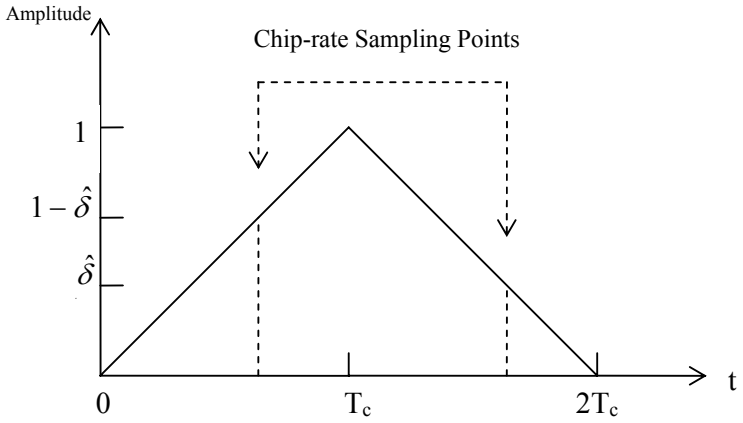

Figure 3.2. Sampling of the chip-matched filter response for rectangular chip pulse. Evident is the error in chip-matched filter response at the sampling points due to time delay mismatch.

3.3.2 Robust MCM Decorrelating Detector

In view of (3.18), the received signal complex vector from (3.3) can be modified as

$$\mathbf{r}_p = \mathbf{S}'_p \widetilde{\mathbf{C}}'_p \mathbf{A}'\mathbf{b}' + \mathbf{n}_p \tag{3.19}$$

where the channel matrix $\widetilde{\mathbf{C}}'_p = \mathbf{I}_2 \otimes \widetilde{\mathbf{C}}_p$, the data vector $\mathbf{b}' = [\mathbf{b}^T \quad \mathbf{b}^T]^T$, and the extended amplitude matrix $\mathbf{A}' = \mathbf{I}_{2M} \otimes \mathbf{a}'$,

$$\begin{aligned}\mathbf{a}' = diag(&a_{1,1} \quad \cdots \quad a_{1,N_T} \quad a_{2,1} \quad \cdots \quad a_{K,1} \quad \cdots \quad a_{K,N_T} \quad (\delta_{1,p} - \hat{\delta}_{1,p})a_{1,1} \quad \cdots \\ &(\delta_{N_T,p} - \hat{\delta}_{N_T,p})a_{1,N_T} \quad (\delta_{1,p} - \hat{\delta}_{1,p})a_{2,1} \quad \cdots \quad (\delta_{1,p} - \hat{\delta}_{1,p})a_{K,1} \\ &\cdots \quad (\delta_{N_T,p} - \hat{\delta}_{N_T,p})a_{K,N_T})\end{aligned}$$

and the extended code matrix

$$\mathbf{S}'_p = [\hat{\mathbf{S}}_{k,n,p}(1) \quad \cdots \quad \hat{\mathbf{S}}_{k,n,p}(M) \quad \Delta\mathbf{S}_{k,n,p}(1) \quad \cdots \quad \Delta\mathbf{S}_{k,n,p}(M)] \tag{3.20}$$

The robust space-time decorrelating detector (RSTD) is then

$$\hat{\mathbf{b}}' = sign\left(\mathrm{Re}\left[\sum_{p=1}^{N_R} [\widetilde{\mathbf{C}}'^{\,H}_p \mathbf{S}'^{\,H}_p \mathbf{S}'_p \widetilde{\mathbf{C}}'_p]^{-1} \widetilde{\mathbf{C}}'^{\,H}_p \mathbf{S}'^{\,H}_p \mathbf{r}_p \right] \right) \tag{3.21}$$

The signal energy in the error vector may be small enough so that we only use the signal energy in the estimated code vector for bit detection, i.e., $\hat{\mathbf{b}} = \hat{\mathbf{b}}'_{[1:KMN_T]}$ where $\hat{\mathbf{b}}'_{[1:J]}$ is a vector consisting of the first J elements of vector $\hat{\mathbf{b}}'$.

By doubling the dimension of the correlation matrix, the RSTD has eight times the complexity of the decorrelator. With each user decomposed into two virtual users, the upper bound on capacity is reduced from L to L/2, where L is the spreading factor.

3.3.3 Multistage Robust MCM Decorrelating Detector

To improve capacity and reduce complexity, a multistage version of the RSTD can be formulated as in [25]. The M error vectors for each transmit antenna of one user are

grouped into one long vector based on the tentative estimated data bits, defined as

$$\mathbf{e}_{k,n,p} = \sum_{m=1}^{M} c_{n,p}\hat{b}_{k,n}^{j+1}(m)\Delta\hat{\mathbf{s}}_{k,n,p}(m),\ k=1,\ \ldots,\ \mathrm{K},\ n=1,\ \ldots,\ \mathrm{N_T}. \tag{3.22}$$

A new code matrix, $\mathbf{S}''_p$, can therefore be constructed with a smaller dimension than that of (3.20)

$$\mathbf{S}''_p = [\hat{\mathbf{S}}_{k,n,p}(1) \quad \hat{\mathbf{S}}_{k,n,p}(2) \quad \cdots \quad \hat{\mathbf{S}}_{k,n,p}(M) \quad \mathbf{e}_{1,1,p} \quad \cdots \quad \mathbf{e}_{K,N_T,p}] \tag{3.23}$$

Data estimation under the multistage RSTD is performed by the following procedure:

Step (1) Use a STD with the estimated timing delay and obtain the initial tentative data bits.

$$\hat{\mathbf{b}}' = sign\left(\mathrm{Re}\left[\sum_{p=1}^{N_R} [\widetilde{\mathbf{C}}''^{H}_{p} \hat{\mathbf{S}}^{H}_{p} \hat{\mathbf{S}}_{p} \widetilde{\mathbf{C}}''_{p}]^{-1} \widetilde{\mathbf{C}}''^{H}_{p} \hat{\mathbf{S}}^{H}_{p} \mathbf{r}_p \right] \right) \tag{3.24}$$

where $\hat{\mathbf{S}}_p$ is defined as in (3.4), but with $\hat{\mathbf{S}}_{k,n,p}(i)$ replacing $\mathbf{S}_{k,n,p}(i)$, and $\widetilde{\mathbf{C}}''_p = diag(\widetilde{\mathbf{C}}_p \quad \mathbf{I}_{KN_T})$.

Step (2) Construct code matrix, $\mathbf{S}''_p$, based on the current tentative data bits using Equations (3.22) and (3.23).

Step (3) Obtain tentative data bits for next stage.

$$\hat{\mathbf{b}}'' = sign\left(\mathrm{Re}\left[\sum_{p=1}^{N_R} [\widetilde{\mathbf{C}}''^{H}_{p} \mathbf{S}''^{H}_{p} \mathbf{S}''_{p} \widetilde{\mathbf{C}}''_{p}]^{-1} \widetilde{\mathbf{C}}''^{H}_{p} \mathbf{S}''^{H}_{p} \mathbf{r}_p \right] \right) \tag{3.25}$$

Step (4) If the change of $\hat{\mathbf{b}}''$ from the previous stage is small, end iteration. Otherwise, go to Step 2.

Capacity of the multistage RSTD detector is now improved to (M/M+1)L. For a moderate frame size of M = 4, capacity approaches 80% of the spreading code length. Correlation matrix size is reduced to $(M+1)KN_T$-by-$(M+1)KN_T$, but computations of

the matrix inversion in (3.24) and (3.25) are still intensive.

3.3.4 Robust MCM SIC Detector

The linear SIC is a computationally attractive iterative implementation of the decorrelating detector. The convergence property of the linear SIC is provided in [32], and is similar to the space-alternating generalized expectation-maximization (SAGE) [39]-based iterative decorrelating detector [40]. Since there is no need for power ordering, a procedure commonly carried out in a multistage detector, the receiver complexity is further reduced. Zha and Blostein [25] proposed an iterative implementation of the multistage robust SIC, and we now extend this detector to a MCM environment. We propose a robust space-time SIC (RSTSIC) that combines the original robust SIC with maximal ratio combining (MRC) of the multiple data streams arriving at each mobile. We also use a more efficient stripping algorithm for the implementation of the original robust SIC. This algorithm is functionally-equivalent as the one proposed in [25], but is more computationally efficient because interfering users' reconstructed signals do not have to be subtracted at each bit-estimate iteration. Instead, the relevant desired signal is estimated and then subtracted away at each iteration from the received signal, thus removing its influence on the composite signal, much akin to an onion-peeling process.

Initialization:

For $1 \le k \le \mathrm{K}$, $1 \le m \le \mathrm{M}$, set:

$$\hat{\mathbf{s}}_{k,n,p}(m) = \hat{\delta}_{n,p}\mathbf{d}_k(\rho_{n,p}+1,m) + (1-\hat{\delta}_{n,p})\mathbf{d}_k(\rho_{n,p},m)$$

$$\Delta\hat{\mathbf{s}}_{k,n,p}(m) = \mathbf{d}_k(\rho_{n,p}+1,m) - \mathbf{d}_k(\rho_{n,p},m)$$

$$\hat{a}_k^0(m) = 0$$

$$\hat{b}_k^0(m) = 0$$

$\Delta\hat{a}_k^0(m) = 0$

Iteration:

For $j = 0,1,\ldots$ do:

For $k = 1,2,\ldots,K$ do:

For $n = 1,2,\ldots N_T$ do:

Steps (A) through (E):

(A): Determine user k's remaining data information for the (j+1)st iteration and update the amplitude and data bits

$$newInfo_{k,n,p}^{j+1}(m) = ((\hat{\mathbf{s}}_{k,n,p}(m))^H (r_p^{j+1}))/\| \hat{\mathbf{s}}_{k,n,p}(m) \| \tag{3.26}$$

$$newInfo_{k,n}^{j+1}(m) = \mathrm{Re}\left[\sum_{p=1}^{N_R} c_{n,p}^* newInfo_{k,n,p}^{j+1}(m) \Big/ \sum_{p=1}^{N_R} c_{n,p}^* c_{n,p} \right] \tag{3.27}$$

$$\hat{a}_{k,n}^{j+1}(m) = abs\left(newInfo_{k,n}^{j+1}(m) + \hat{a}_{k,n}^{j}(m)\hat{b}_{k,n}^{j}(m)\right) \tag{3.28}$$

$$\hat{b}_{k,n}^{j+1}(m) = sign\left(newInfo_{k,n}^{j+1}(m) + \hat{a}_{k,n}^{j}(m)\hat{b}_{k,n}^{j}(m)\right) \tag{3.29}$$

where $\|\cdot\|$ denotes the conventional 2-norm function, while $abs(\cdot)$ and $sign(\cdot)$ denote absolute value and the sign, respectively. Despreading of the signature waveform is done in (3.26), and we perform the MRC step here in (3.27) by weighing each transmit-receive signal pair by their respective channel gain coefficients. After combining, the signal is normalized by the sum of channel gains so that amplitude information can be estimated.

(B): Update the estimate of the remaining received signal

$$\hat{\mathbf{r}}_{k,n,p}^{j+1} = \sum_{m=1}^{M} c_{n,p} newInfo_{k,n}^{j+1}(m)\hat{\mathbf{s}}_{k,n,p}(m) \tag{3.30}$$

Note that only the currently extracted information is used for signal reconstruction. The nature of the MIMO channel is also taken into account in this step by the multiplication of the channel coefficient to ensure proper

self-interference cancellation.

(C): Estimate the residual signal of the *k*th user due to timing error as

$$\Delta \mathbf{r}_{k,n,p}^{j+1} = \mathbf{r}_{p}^{j} - \hat{\mathbf{r}}_{k,n,p}^{j+1} + \Delta \hat{\mathbf{a}}_{k,n,p}^{j} \mathbf{e}_{k,n,p}^{j} \tag{3.31}$$

(D): Update the amplitude of the error vector

$$\mathbf{e}_{k,n,p}^{j+1} = \sum_{m=1}^{M} c_{n,p} \hat{b}_{k,n}^{j+1}(m) \Delta \hat{\mathbf{s}}_{k,n,p}(m) \tag{3.32}$$

$$\Delta \hat{\mathbf{a}}_{k,n,p}^{j+1} = \mathrm{Re}[(\mathbf{e}_{k,n,p}^{j+1})^{H} (\Delta \mathbf{r}_{k,n,p}^{j+1}) / (c_{n,p}^{*} c_{n,p} \parallel \mathbf{e}_{k,n,p}^{j+1} \parallel)] \tag{3.33}$$

For error vector reconstruction, each bit interval is multiplied by the channel gain coefficient so that proper weight is accounted for in error vector amplitude estimation. The error vector amplitude is then normalized by channel gain coefficients and averaged over M bits.

(E): Strip away newly extracted information by subtracting the estimated remaining signal and the estimated error signal

$$\mathbf{r}_{p}^{j+1} = \mathbf{r}_{p}^{j} - \hat{\mathbf{r}}_{k,n,p}^{j+1} - c_{n,p} \Delta \hat{\mathbf{a}}_{k,n,p}^{j+1} \mathbf{e}_{k,n,p}^{j+1} \tag{3.34}$$

If for all k = 1 to K , n = 1 to N_T and m = 1 to M, $| \hat{a}_{k,n}^{j+1}(m) - \hat{a}_{k,n}^{j}(m) |$ are below a threshold, end the calculation. Appendix A contains the complete Matlab code of the RSTSIC for a MCM system with $N_T = N_R = 2$.

To improve performance under timing mismatch, the SISO robust SIC employs an error vector estimation and cancellation procedure in conjunction with linear SIC. The interference from timing errors can completely cancelled if the tentative data estimates are correct, otherwise the estimated error vector will be cancelled with amplitude smaller than the true value, leaving residual error signal. Although convergence to the multistage robust decorrelator is not guaranteed, good performance from the robust SIC can be expected as the residual signals from strong interferers are likely to be accurately estimated and cancelled. Moreover, the robust

SIC may even achieve superior performance than that of the multistage robust decorrelator at the intermediate stages where interference is accurately estimated and cancelled. Compared to the SISO case, note that in the proposed RSTSIC, we further apply MRC in (3.27), improving performance through receiver diversity. Spatial self-interference and temporal MAI are separated concurrently by the SIC procedure, in addition to timing error estimation and compensation. The single-antenna robust SIC requires a decorrelating initial stage to combat self-interference when the standard deviation of timing estimation error, σ_T, is greater than $0.2T_C$, else the receiver will be rendered useless [25]. However, due to receiver diversity benefits, the RSTSIC is shown to be delay-error estimate resistant even without an initial decorrelating stage.

3.4 Amplitude Averaging and Soft-Decision Interference Cancellation

In the linear SIC, amplitude information is estimated on a bit by bit basis, along with the data bit estimate. Both estimates are then used for signal regeneration and finally interference cancellation. The signal amplitude, however, is subject to corruption by noise, fading, and MAI. The estimation error can be modeled as AWGN noise, and by averaging the amplitude estimates over M bits, it is shown in theory [41] that the noise variance can be reduced by a factor of M; hence improving performance correspondingly. Convergence of such a smoothing procedure, however, is not guaranteed.

Bit decision functions play an important role in SIC-type algorithms. The hard limiter [42], shown in Fig. 3.3a, makes a bit decision depending on the sign of the receiver soft bit estimate. Although a hard limiter will prevent noise enhancement, error propagation can be introduced. If, for example, noise due to MAI, AWGN and

fading causes a positive bit to become negative, the hard limiter will decide that a negative bit is detected. This will amplify noise, leading possibly to error propagation.

The linear decision function in Fig. 3.3b bases its output on the amplitude and sign of the receiver soft bit estimate [42]. A SIC employing linear bit-decision converges to the decorrelator as the number of interference stages goes to infinity. Therefore, inherent noise enhancement of the decorrelator is also the main drawback of the linear decision function.

Zha and Blostein [43] proposed a generalized clipper decision function to improve the trade-off between the noise enhancement of the linear decision and error propagation of the hard limiter. Fig. 3.3c shows the decision region of the generalized clipper, characterized by the function

$$\hat{b} = \begin{cases} 1, & \widetilde{b} > c \\ \widetilde{b}, & -c < \widetilde{b} < c \\ -1, & \widetilde{b} < -c \end{cases} \tag{3.35}$$

where $\widetilde{b}$ is the receiver soft bit estimate. When the value of the normalized soft bit is smaller than the clipping value, c, linear bit decision will be made since its reliability is in doubt. Otherwise, a hard bit decision will be made for the highly-reliable soft bit. The performance of this decision function is analysed in [43], and it is shown that similar performance can be obtained for a wide range of values of the clipping threshold, c.

3.4.1 Soft-Decision RSTSIC with Amplitude Averaging

Steps (A) and (B) of the RSTSIC are modified to the following steps for amplitude averaging and soft decision interference cancellation.

(a): Determine user k's remaining soft data information for the (j+1)st iteration and

update the soft amplitude and data bits

$$newInfo_{k,n,p}^{j+1}(m) = ((\hat{\mathbf{s}}_{k,n,p}(m))^H (r_p^{j+1}) \big/ \| \hat{\mathbf{s}}_{k,n,p}(m) \| \tag{3.36}$$

$$newInfo_{k,n}^{j+1}(m) = \mathrm{Re}\left[\sum_{p=1}^{N_R} c_{n,p}^* newInfo_{k,n,p}^{j+1}(m) \Big/ \sum_{p=1}^{N_R} c_{n,p}^* c_{n,p} \right] \tag{3.37}$$

$$\tilde{a}_{k,n}^{j+1}(m) = abs\left(newInfo_{k,n}^{j+1}(m) + \hat{a}_{k,n}^{j}(m)\hat{b}_{k,n}^{j}(m) \right) \tag{3.38}$$

$$\tilde{b}_{k,n}^{j+1}(m) = sign\left(newInfo_{k,n}^{j+1}(m) + \hat{a}_{k,n}^{j}(m)\hat{b}_{k,n}^{j}(m) \right) \tag{3.39}$$

(b): Calculate the average amplitude

$$\bar{a}_{k,n}^{j+1} = \frac{1}{M} \sum_{m=1}^{M} \tilde{a}_{k,n}^{j+1}(m) \tag{3.40}$$

(c): Perform soft bit decision using (3.35)

$$\hat{a}_{k,n}^{j+1}(m)\hat{b}_{k,n}^{j+1}(m) = \begin{cases} \bar{a}_{k,n}^{j+1}\tilde{b}_{k,n}^{j+1}(m), & \tilde{a}_{k,n}^{j+1}(m) / \bar{a}_{k,n}^{j+1} > c \\ \tilde{a}_{k,n}^{j+1}(m)\tilde{b}_{k,n}^{j+1}(m), & \tilde{a}_{k,n}^{j+1}(m) / \bar{a}_{k,n}^{j+1} < c \end{cases} \tag{3.41}$$

Here we use the average amplitude as the normalizing constant for the soft decision. The soft amplitude whose normalized value is greater than *c* is hard-limited to the amplitude average. Otherwise, a linear decision is used for the amplitude estimation.

(d): Update the estimate of the received signal

$$\hat{\mathbf{r}}_{k,n,p}^{j+1} = \sum_{m=1}^{M} c_{n,p} \hat{a}_{k,n}^{j+1}(m)\hat{b}_{k,n}^{j+1}(m)\hat{\mathbf{s}}_{k,n,p}(m) \tag{3.42}$$

Note that the estimated received signal is composed of the total amount of extracted information, as opposed to the information extracted at the *j+1*th iteration in the algorithm in Section 3.3.4. Therefore, $\hat{\mathbf{r}}_{k,n,p}^{j}$ has to be added back to the signal $\mathbf{r}^j$ before performing residual signal ($\Delta\mathbf{r}_{k,n,p}^{j+1}$) estimation.

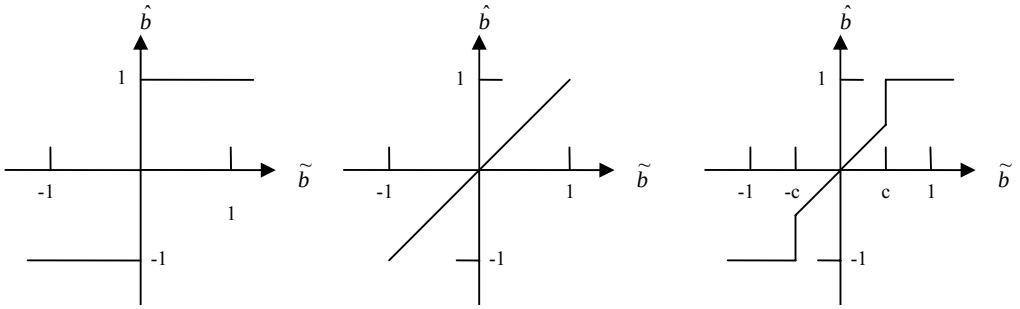

a) hard decision b) linear decision c) generalized clipper

Figure 3.3. Decision functions

3.5 Performance Analysis

3.5.1 BER

The output of the STD at the *p*th receive antenna is denoted by

$$\begin{aligned} \mathbf{d}_p &= \mathbf{R}_p^{-1}\widetilde{\mathbf{C}}_p^H\mathbf{S}_p^H\mathbf{r}_p \\ &= \mathbf{A}\mathbf{b} + \widetilde{\mathbf{n}}_p \end{aligned} \tag{3.43}$$

where the covariance matrix of $\widetilde{\mathbf{n}}_p$ is $\sigma^2\mathbf{R}_p^{-1}$ and $\mathbf{R}_p = \widetilde{\mathbf{C}}_p^H\mathbf{S}_p^H\mathbf{S}_p\widetilde{\mathbf{C}}_p$.

We can minimize the error probability by maximal ratio combining the STD outputs and obtain the bit estimates

$$\hat{\mathbf{b}} = sign\left(\mathrm{Re}\left[\sum_{p=1}^{N_R} \mathbf{R}_p^{-1}\widetilde{\mathbf{C}}_p^H\mathbf{S}_p^H\mathbf{r}_p \right] \right) \tag{3.44}$$

and the decision statistic can be written as

$$\mathrm{Re}\left[\sum_{p=1}^{N_R} \mathbf{R}_p^{-1}\widetilde{\mathbf{C}}_p^H\mathbf{S}_p^H\mathbf{r}_p \right] = \mathbf{A}\mathbf{b} + \overline{\mathbf{n}} \tag{3.45}$$

where the covariance of the zero-mean Gaussian random vector $\overline{\mathbf{n}}$ is

$$E[\mathbf{n}^T\mathbf{n}] = \frac{1}{2}\sigma^2 \sum_{p=1}^{N_R} \mathbf{R}_p^{-1} \tag{3.46}$$

The probability of error, conditioned on $\widetilde{\mathbf{C}}_p$ and $\mathbf{S}_p$, of the STD detector with perfect time delay of the *i*th bit for the *j*th substream of the *k*th user is [44]

$$P_{i,j,k|\mathbf{C}_p,\mathbf{S}_p}(\sigma) = Q\left(\frac{a_k}{\frac{1}{\sqrt{2}}\sigma\sqrt{\sum_{p=1}^{N_R} \mathbf{R}_{p\,[(i-1)KN_T+(j-1)K+k]}^{-1}}} \right) \tag{3.47}$$

where $\mathbf{R}_{p\,[(i-1)KN_T+(j-1)K+k]}^{-1}$ denotes the [*(i-1)KN*$_T$*+(j-1)K+k*]th diagonal of the matrix $\mathbf{R}_p^{-1}$, a_k is the received signal energy of user *k*, σ is the standard deviation of white Gaussian noise, and $Q(x) = \frac{1}{\sqrt{2\pi}}\int_x^\infty e^{-(t^2/2)}dt$. MAI is accounted for in (3.47) in the $\mathbf{S}_p$ code matrix, which is dependent on the time-delay of the signals arriving at antenna *p*. The average BER for user *k* is then calculated by simulating a large number of realizations of $\widetilde{\mathbf{C}}_p$ and $\mathbf{S}_p$**,** and averaging the BER over a frame of M bits and N_T substreams to obtain the final value. Note that in (3.47) we do not make any explicit assumptions about the distributions of the channel and timing error random variables. The Q-function in the error probability expression arises only from the assumption that the noise is Gaussian.

For the RSTD with perfect time-delay estimates, the BER can be obtained as (3.47) with $\mathbf{S}_p$ and $\widetilde{\mathbf{C}}_p$ replaced by $\mathbf{S}_p^{'}$ and $\widetilde{\mathbf{C}}_p^{'}$ respectively, from Section 3.3.2.

To compute the exact probability of error for the RSTSIC given a specific timing error, a total of 2^{MKN_T-1} Q-functions must be calculated and summed [19]. Moreover, a large number of instances of time-delay errors and the flat fading channel have to be averaged to obtain the BER. Therefore, the computation of the exact BER is almost

impossible in practice even for modest values of M, K and N_T. However, given that the RSTSIC is an iterative implementation of the multistage RSTD, we can use the previously derived BER of the RSTD as an upper bound. This is because the multistage RSTD is, in effect, an iterative implementation of the RSTD with fewer interfering users. Therefore, the multistage RSTD is expected to have a superior performance over the RSTD. The BER of the RSTSIC with perfect soft data estimates would, therefore, be upper-bounded by the RSTD with perfect time-delay information.

3.5.2 Implementation Complexity

In this subsection we analyze the computational complexity of the multiuser CDMA MIMO linear SIC, and further extend it to the RSTSIC case. Comparison to other MCM receivers will also be made.

Assuming convergence in J stages, the linear SIC for CDMA system is of complexity $O(JMLK)$ [32]. For the MCM system case, we can view the total number of users to be KN_T, and for each bit of each user, despreading and signal reconstruction is done for each of the N_R receiving branches. Therefore, the MCM linear SIC is of complexity $O(JMLKN_TN_R)$. In the RSTSIC, each user is decomposed into two virtual users, which, in effect, roughly doubles the number of computations of that of the MCM linear SIC. Thus, the RSTSIC is also of complexity $O(JMLKN_TN_R)$, assuming that the number of SIC stages is the same as that of the MCM linear SIC.

The decorrelator for CDMA has complexity $O(M^3K^3)$ [44], and the STD, which is equivalent to a decorrelator with KN_T users, is of complexity $O(M^3K^3N_T^3)$. The

robust decorrelator doubles the number of users of that of the decorrelator, while the RSTD doubles that of the STD. Therefore, the RSTD also has complexity $O(M^3K^3N_T^3)$.

While the RSTSIC approximately doubles the complexity of that of the MCM linear SIC, its complexity is still far less than those of other MCM receivers. This makes the RSTSIC an ideal downlink receiver where intensive computations should be limited at the mobile receiver.

Chapter 4

Simulation Results

In this section, we evaluate the performance of various multiuser CDMA MIMO (MCM) receivers. The BER performance of the proposed MCM detectors will be compared to other MCM detectors with and without perfect timing delay estimates are presented. Table 4.1 summarizes the MCM receivers studied in this chapter, listing their acronyms, unabbreviated names, and respective references.

Unless otherwise stated, we will assume that both the mobile and basestation have two antennas, i.e. $N_T = N_R = 2$. We assume N_T independent data streams of one user will be spread by the same Gold code [45] of length 31, and transmitted through the N_T transmit antennas. A frame size of M = 4 is used, while the near-far ratio (NFR), defined as the power ratio between the strongest interferer and the desired user, is fixed at 20dB. Without loss of generality, we assume that the user of interest is the first user, who also has the weakest power. All other interferers have power uniformly distributed between the strongest interferer and the desired user. As in [25], the delay estimation errors are modelled as independent zero-mean Gaussian random variables with equal standard deviation $\sigma_T = 0.1T_C$ for all users. Timing delay estimates are assumed to have fractional uncertainty only, while data bits are BPSK modulated and rectangular chip pulses are used for spreading. When using the generalized clipper

Acronym	Unabbreviated Name	Reference
STD	Space-Time Decorrelator	3.2.1
V-BLAST	Vertical Bell Labs Layered Space-Time	2.2.3 [26]
STD+VBLAST	Space-Time Decorrelator plus V-BLAST	3.2.1 [27]
LAST-MUD	Layered Space-Time MultiUser Detector	3.2.3 [29]
RSTD	Robust Space-Time Decorrelator	3.3.2
RSTSIC	Robust Space-Time Successive Interference Canceller	3.3.4

Table 4.1. List of MCM receiver acronyms used in this Chapter.

decision function, we set $c = 0.5$ for the clipping threshold, which is found to be optimum for SISO systems [43]. We also expect this value of clipping threshold to perform well in the MCM system since the steady-state performance of the clipping threshold relative to single-user performance is similar for a wide range of values.

We use an error-counting process to generate the BER curves in our simulations. The number of errors required to end the simulation for a desired user is $10MN_T$, or 1000 Monte-Carlo runs, whichever one comes later. The BER is then calculated by averaging over the number of substreams and frame size.

4.1 Single-User vs. MCM Detectors in a Multiuser Environment

In Fig. 4.1, we examine the performances of conventional single-user point-to-point MIMO receivers in a multiuser environment with K = 5 users. In a perfectly power-controlled MCM system, the conventional V-BLAST receiver reaches an error floor at

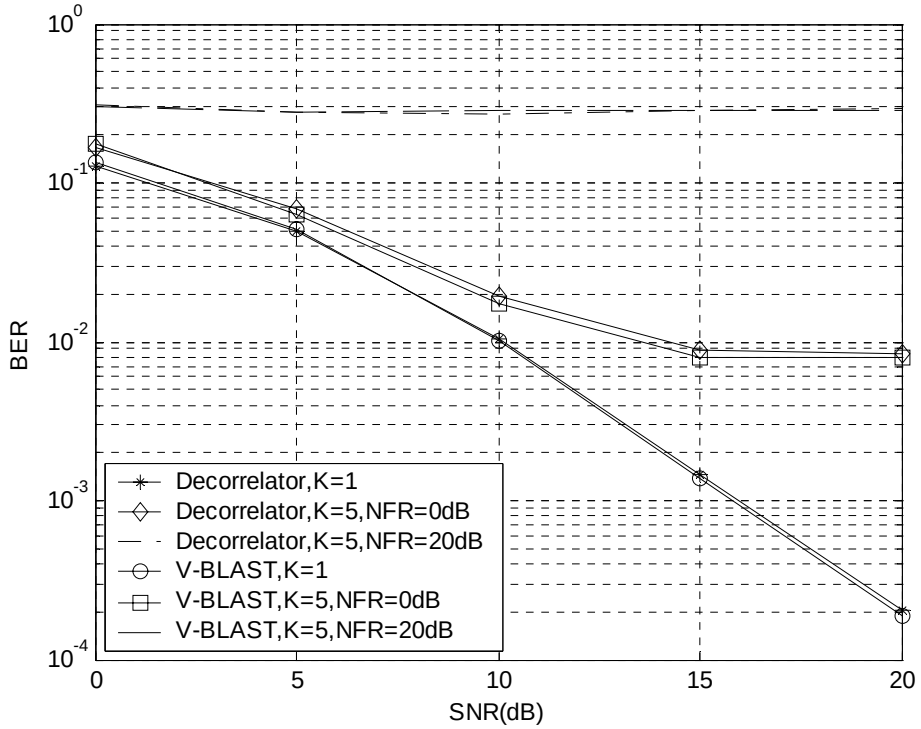

Figure 4.1. The BER of single-user receivers in multiuser environment with perfect timing estimation.

a BER of $8x10^{-3}$. Furthermore, in a near-far scenario with NFR of 20 dB, the V-BLAST is rendered useless as its BER cannot dip below $2x10^{-1}$. The performance degradation due to MAI from the multiple transmit antennas is therefore far too great to be ignored. For reference, we compare to a single-user environment, where we find that V-BLAST performs slightly better than the decorrelator as expected, since V-BLAST is an iterative, post-detection SNR-maximizing implementation of the decorrelator. Fig. 4.2 shows the performance improvement of the STD+VBLAST receiver introduced in Section 3.2 over the traditional V-BLAST receiver. With NRF = 20 dB, the STD+VBLAST receiver is able to attain single-user performance with K = 5 users. Therefore, we see enormous potential benefits in a highly spectral-efficient MCM system.

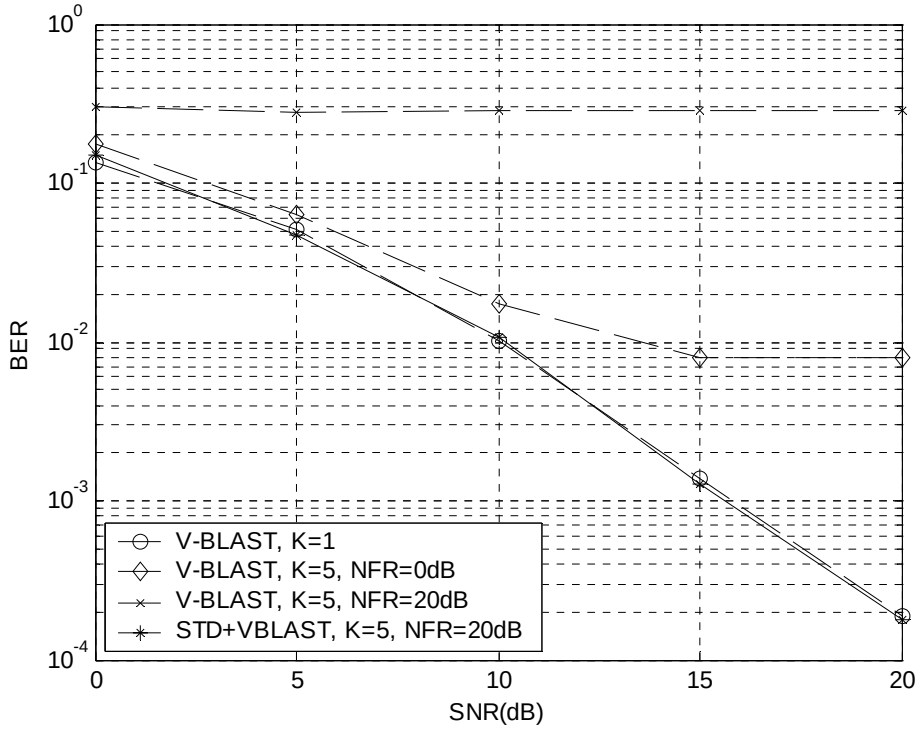

Figure 4.2. BER comparison of STD+VBLAST and single-user V-BLAST receivers in a multiuser environment with perfect time estimation.

4.2 Impact of Timing Estimation Errors

We next examine the impact of timing estimation error on the performance of the MCM receivers of Section 3.2 in Fig. 4.3. With perfect time-delay estimates, all three receivers perform similarly for K = 5 users, with LAST-MUD edging out STD and STD+VBLAST. Single-user V-BLAST performance is attained by all three MCM detectors in this case. The BER of all three MCM receivers exhibit signs of flooring at an SNR of 10 dB when timing estimates are used for detection instead of true timing values. Note that in a single-user system, timing estimation error does not have a significant effect on the performance of the V-BLAST receiver, as shown in Fig. 4.4. However, in a multiple-access scenario, as created by the multiple antennas,

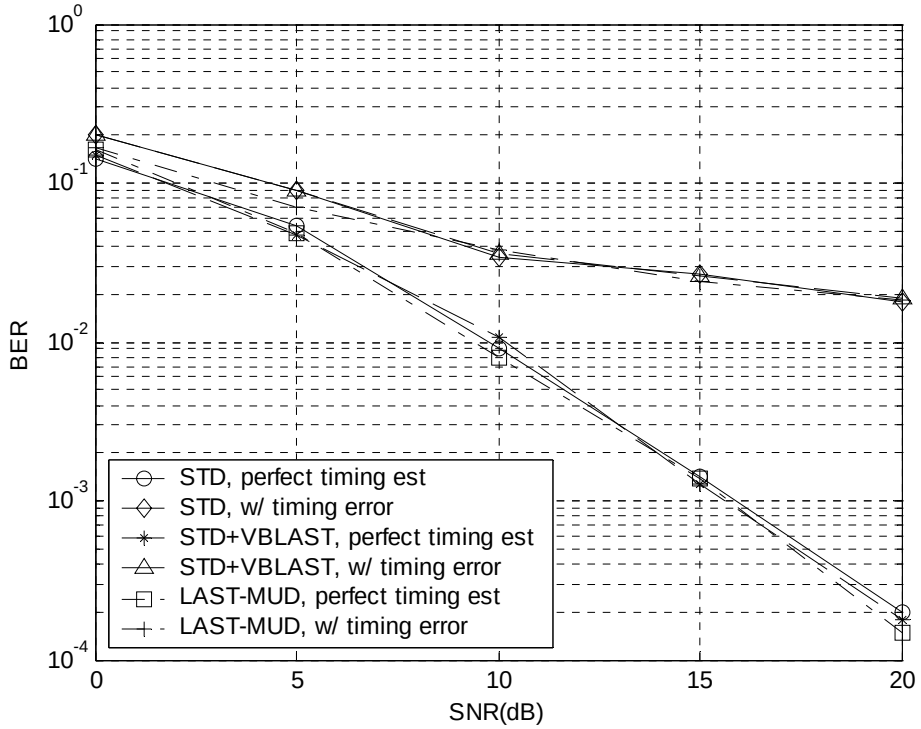

Figure 4.3. BER of MCM receivers with and without timing estimation errors for K = 5 users.

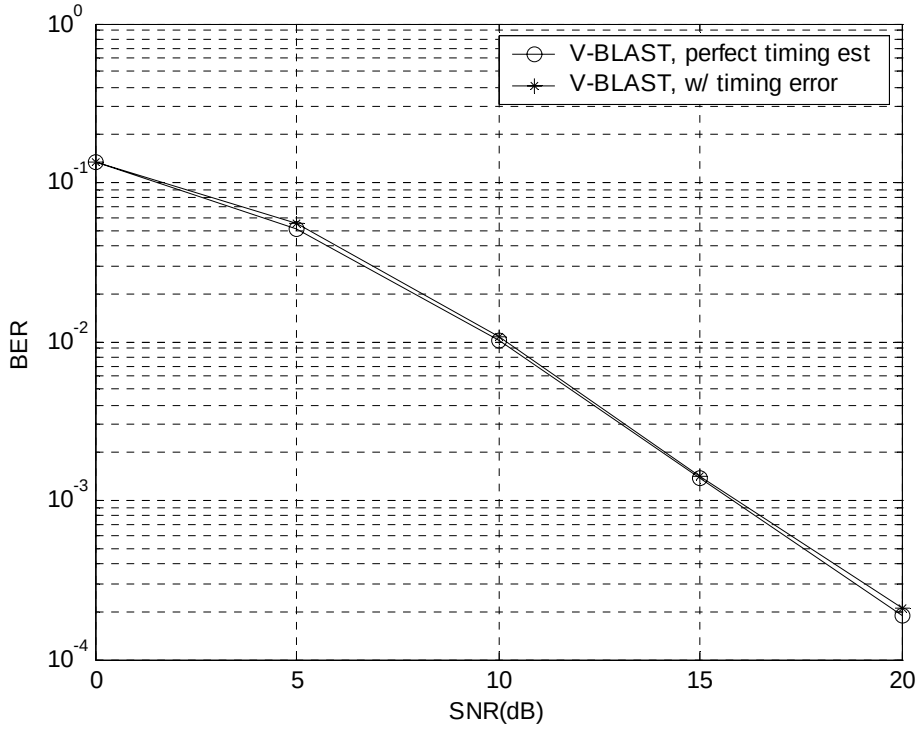

Figure 4.4. The BER of single-user V-BLAST detector with timing estimation error in a single-user environment, i.e. K = 1.

timing estimation error induces more MAI, invoked by the increase in cross-correlation between the PN codes and smaller auto-correlation values due to timing mismatch.

4.3 Robust to Timing MCM Detectors

Fig. 4.5 compares the performances of STD, RSTD, and RSTSIC of Chapter 3 under perfect and imperfect timing estimates. The LAST-MUD and STD+VBLAST are not shown here since their performances are similar to that of STD. In the case where the number of users in the system is K = 5, the RSTSIC outperforms the RSTD by more than 7 dB, and is close to that of the ideal STD. At a BER of 10^{-3}, the loss of RSTSIC in comparison to the STD with perfect timing estimate is about 1 dB, whereas the BER of the STD with estimated timing levels off at around 10^{-2} at high SNR. The proposed RSTSIC is found to converge within 10 iterations on average, where we define convergence to occur when the difference in estimated amplitude value between two consecutive iterations is less than 1%. The RSTSIC therefore provides considerable performance gain in comparison to the RSTD, while avoiding the computationally intensive matrix inversions required in the decorrelator-type receivers.

In Fig. 4.6, the performance of the RSTSIC under various system loads is shown. We observe that BER within 2.5 dB of single user performance is attained when the number of users is less than 10, while at SNR = 20 dB, the BER is showing signs of flooring for K = 15 users. The first 10 users suffer very little performance loss, but increasing by another 10 users causes the RSTSIC to break down. As we will see in

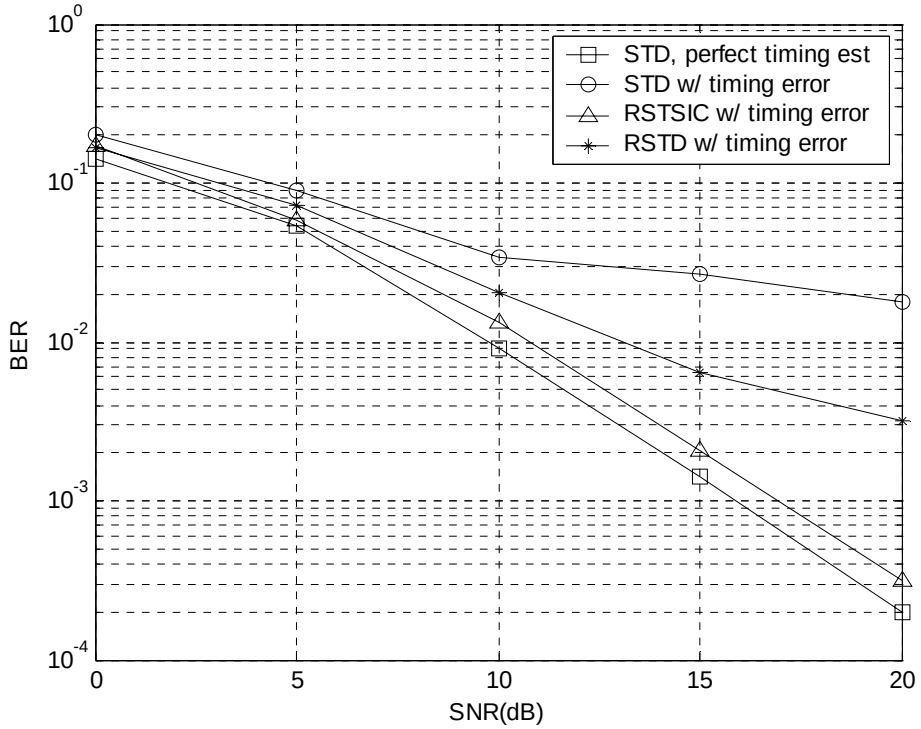

Figure 4.5. Performance comparison between RSTSIC, RSTD and STD with and without timing mismatch for K = 5 users.

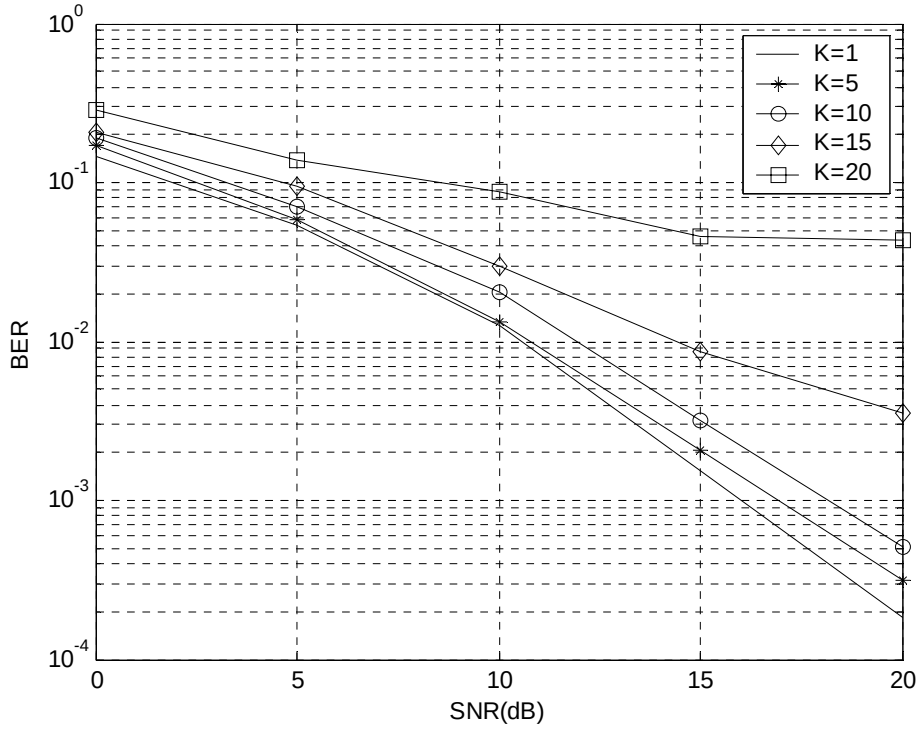

Figure 4.6. Performance of RSTSIC under various user loads.

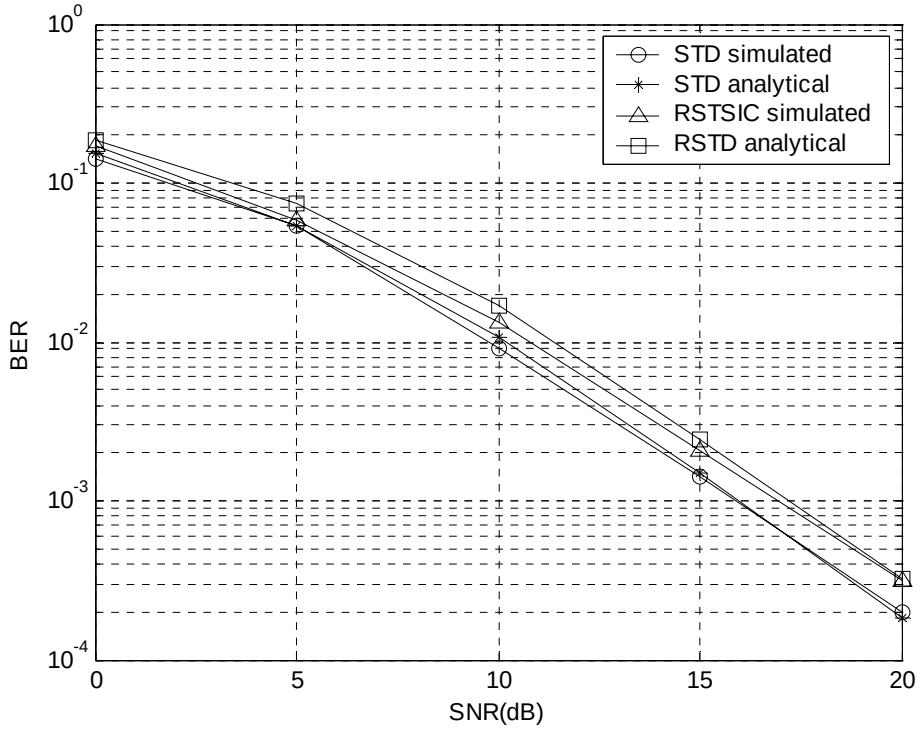

Figure 4.7. Comparison of analytical and simulation results for K = 5 users.

Section 4.8, by reducing noise enhancement and error propagation using amplitude averaging and a generalized clipper decision function, performance can be dramatically improved for the RSTSIC.

To verify our simulation results, analytical BER performances of the STD and RSTD with perfect time-delay estimations are shown in Fig. 4.7. The RSTD serves as the upper bound for the linear-decision RSTSIC for reasons mentioned in Section 3.5.1. The simulated STD BER conforms closely to the analytical results, while the RSTSIC is shown to be bounded by the RSTD, as expected, since this particular scenario has very few interferers.

4.4 Performance of the RSTSIC under Large Delay Variance

Fig. 4.8 shows a plot of the BER for both RSTSIC and RSTD as a function of the values of delay estimation error deviation σ_T, varying from 0 to T_C in increments of $0.1T_C$, and the SNR is fixed at 15 dB. Note that interfering users' timing delays are the same as that of the desired user, as all signals are transmitted from the same basestation and received at the same mobile. Assuming the user is under acquisition, the delay error is truncated to within $\pm 0.5T_C$ of the true delay. At high σ_T, the delay error is $0.5T_C$ with high probability, representing a worst-case scenario with the greatest signal energy loss [13]. The RSTD performance starts to degrade rapidly when $\sigma_T \geq 0.1T_C$, while the RSTSIC is quite insensitive to the value of σ_T, although slight performance drop is seen as σ_T increases. This is in contrast to the robust decorrelator (RD) and robust SIC in [25], in which the performance of the RD is invariant to the value of σ_T, and the robust SIC required a decorrelating first stage to stay at par with the performance of the RD when $\sigma_T \geq 0.2T_C$. Adding a decorrelating first stage to the robust SIC as proposed in [25] provides little performance gain for the RSTSIC, and therefore is not considered because of the added complexity. From the results shown here, we conclude that receiver diversity has helped RSTSIC to combat large timing estimation errors.

4.5 Spectrally-Efficient Transmission Strategies

It is shown in [33] that the capacity of a MCM system grows linearly with the number of antennas as in the single user system. By using a simple receive diversity

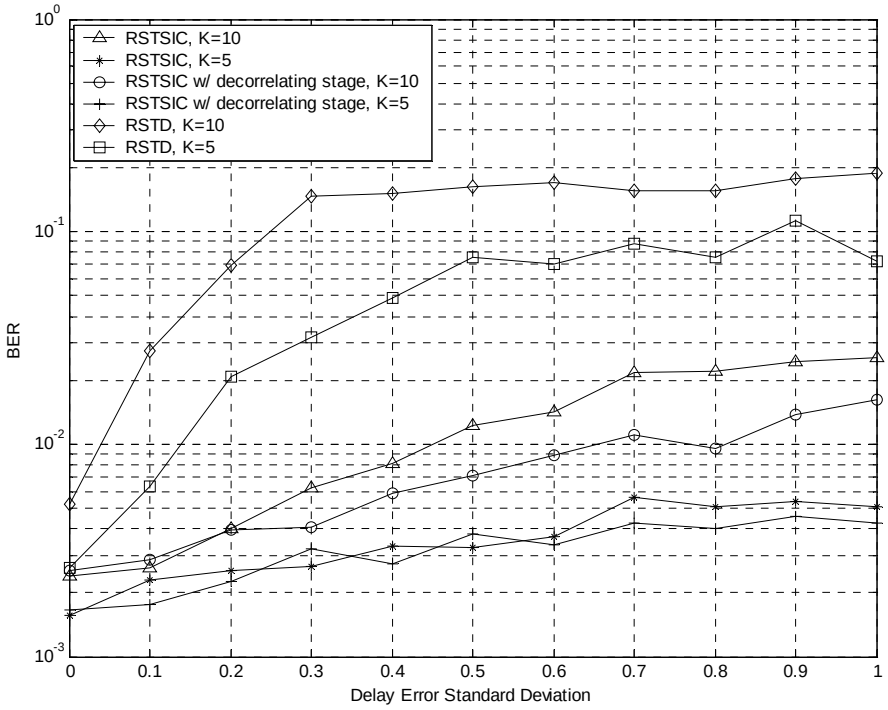

Figure 4.8. The BER as a function of σ_T for RSTSIC and RSTD, with SNR = 15 dB.

technique, MRC, system capacity increases linearly with the number of receive antennas, up to the PN code limit. Note that the increase in capacity in this case is independent of transmit diversity order, in contrast to the V-BLAST result which states that the system capacity increases linearly with the minimum of the number of transmit and receive antennas [33]. Beyond the code limit, the ability to spatially separate desired user's streams and temporally remove MAI is vital to linear capacity growth. Therefore, in a heavily loaded system, either increasing spreading gain or increasing the number of receive antennas may be required to reach acceptable error rates. Increasing the number of receive antennas on a mobile is impractical, while larger spreading codes reduce the spectral efficiency. To avoid increasing the bandwidth of the system due to increasing spreading length, the system can reduce the

data rate of users by decreasing the number of data streams. This will reduce the amount of MAI or self-interference depending on which user's stream is cut back.

4.6 Spreading Code Assignment

One interesting and important issue to investigate is the assignment of spreading codes for the transmit antennas among the multiple users in the CDMA MIMO system. Because bandwidth is a limited resource, its efficiency of usage is of utmost importance. Therefore, we wish to maximize the capacity of the system given a fixed amount of bandwidth, i.e. spreading gain. Intuitively, using different spreading codes on all antennas for all users in the system will result in the best BER performance. For L = 31, the total number of available Gold codes is 33. Assume that each user has two data streams, each spread by a different spreading code, the total number of users that can be supported is 16. Therefore, in a system with more than 16 users, one could use either the same Gold code for all streams of one user, or different random codes for all streams of all users. It is not clear which code usage would result in a better BER performance, thus we examine the above-mentioned scenario in Fig. 4.9 for K = 20 users. The PN sequences of random codes are antipodal binary sequences generated independently, and a different sequence is generated for each simulation run. Therefore, selection of random codes with good cross- and/or auto-correlation properties is not performed, and the performance shown here is the average of many non-optimized random codes. High cross-correlation of random codes may account for the poor performance that we observe. When L = 31, random codes cannot be used to provide adequate near-far resistance. As the spreading length increases to L = 63, the random code performance approaches that of the Gold codes due to lowered

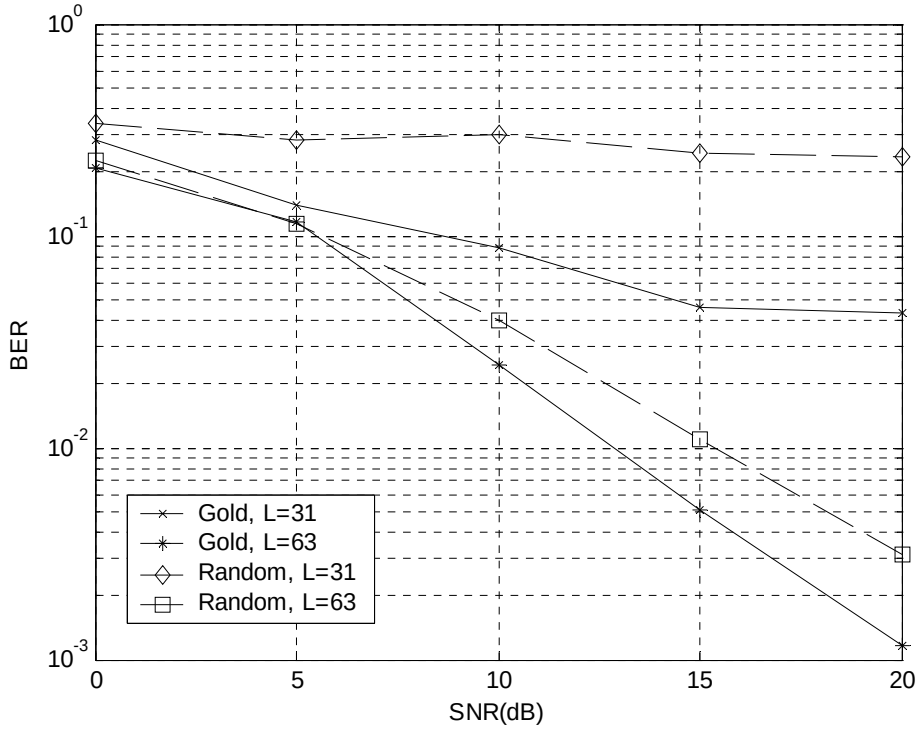

Figure 4.9. Comparison of RSTSIC when using Gold or random codes for K = 20 users.

cross-correlation, which is calculated to be $1/3L$ in [44] for asynchronous channels. However, about 2.5 dB is still lost by using random codes. Therefore, when the code capacity limit is reached, it is desirable to use the same Gold codes for all streams of one user. Fig. 4.10 compares the performance difference between using the same spreading code for all streams of one user and using different codes for all streams of one user. From the figure, we see that marginal performance is gained by using different codes on separate streams as spatial multiplexing is able to effectively separate the temporally correlated data streams. Therefore, in a rich-scattering environment with independent fading, the same spreading code should be used for all data streams of one user to maximize the spectral efficiency of the system.

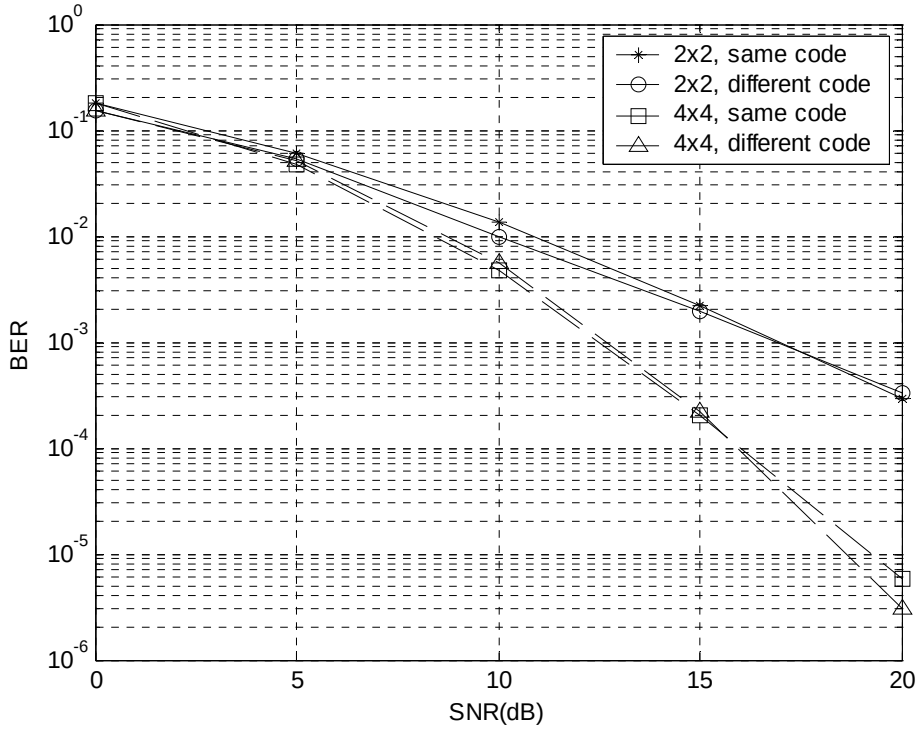

Figure 4.10. Performance of the RSTSIC under various transmission strategies for K = 5 users.

4.7 Varying the Numbers of Antenna Elements

We demonstrate the improvement in capacity by increasing the number of transmit and receive antennas for the RSTSIC in Fig. 4.11. In the following, we denote a system with N_T transmit antennas and N_R receive antennas as N_TxN_R.

We first analyze the performance improvement attained with receiver diversity. While fixing the number of transmit antennas, when going from a 1x1 to a 1x2, a significant gain of 11dB in SNR is obtained at a BER of $4x10^{-3}$. Doubling the number of receive antennas again to 1x4 results in a gain of 6dB over the 1x2 at a BER of $4x10^{-3}$. Diminishing returns will be observed as we increase the number of receiver antennas. We see that by taking advantage of receiver diversity that combines each received signal optimally, significantly lower BER is achieved.

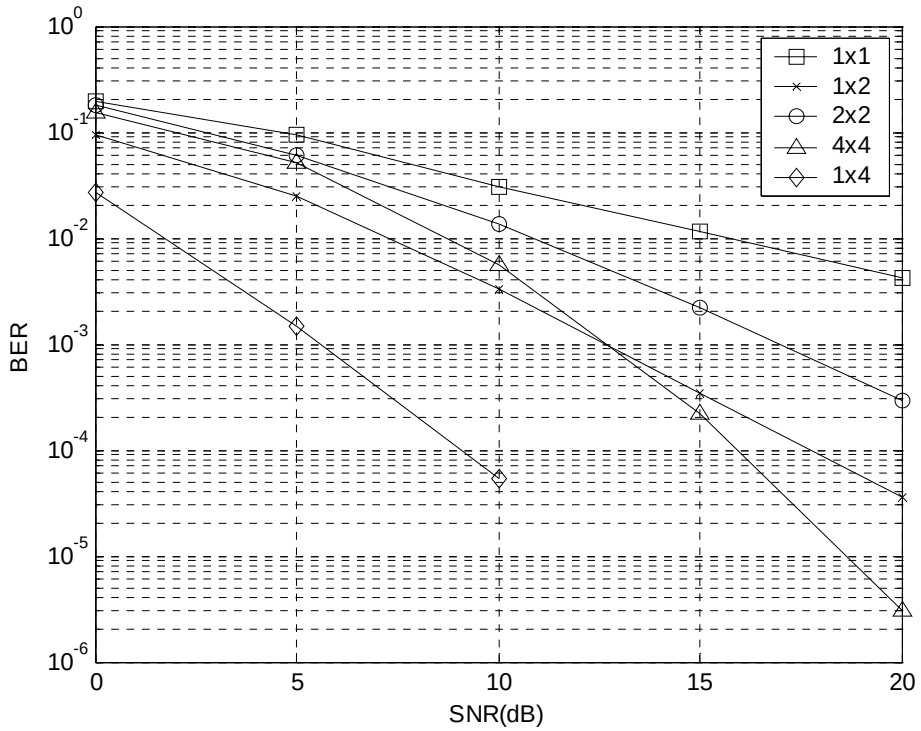

Figure 4.11. The BER of STDSIC under various numbers of transmit and receive antennas elements, where the number of users is K = 5.

Now consider the effects of increasing the number of transmit antennas while the number of receive antennas stay the same. Doubling the number of transmit antennas, and hence data throughput, from a 1x2 to a 2x2 system suffers about 5dB loss at BER of $3x10^{-4}$. Note that the total transmit power is constant as we increase the number of transmit antennas. At approximately 12.5 SNR and $9x10^{-4}$ BER, the 1x2 and 4x4 curves intersect. The throughput is quadrupled by doubling the receiver antennas from two to four at this point of intersection. We are able to achieve this feat because the noise at high SNR is mainly due to MAI, and since we have assumed independent fading and perfect channel gain estimation, the 4x4 receiver is more capable of spatially separating the substreams with increasing diversity.

Therefore, we see that capacity can be increased significantly by increasing the

number of receive antennas and utilizing MRC, while throughput can be increased by transmitting independent data streams over different antennas, at a cost of higher BER. It would be up to the system designer to balance these tradeoffs to meet a particular system requirement.

4.8 Performance of the RSTSIC with Amplitude Averaging and Soft-Decision Function

Fig. 4.12 shows the performance improvement of implementing amplitude averaging and the generalized unit-clipper decision function proposed in [43]. The number of users is K = 15, and the clipping threshold is c = 0.5. We see that using the generalized unit-clipper combined with amplitude averaging produces a BER within 1 dB of the STD with perfect timing estimation, whereas the linear decision function is over 11 dB worse.

In Fig. 4.13, we show the BER under various user loads when implementing the generalized clipper instead of the linear decision function. The BER for K = 15 users using the generalized clipper is within 0.4 dB of the BER for K = 5 users using the linear decision, and an improvement of over 6 dB better when comparing K = 20 users to K = 15 users using the generalized clipper and the linear decision function, respectively.

Fig. 4.14 revisits the performance of the RSTSIC under increasing timing estimate error standard deviation. This time amplitude averaging and the generalized clipper decision function are employed. A similar trend is presented here as in Fig. 4.8, with the curves shifted lower. Therefore, we see that the change in the decision function does not affect the robustness of the RSTSIC against larger standard deviation of the timing estimation error.

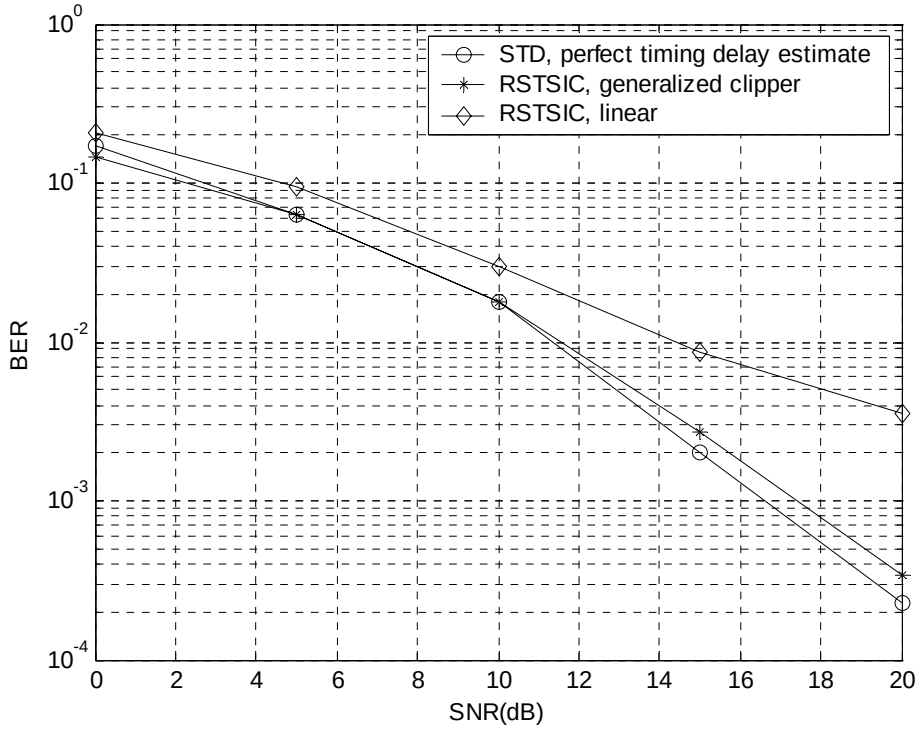

Figure 4.12. Performance comparison of the RSTSIC employing linear or generalized clipper decision functions for K = 15 users.

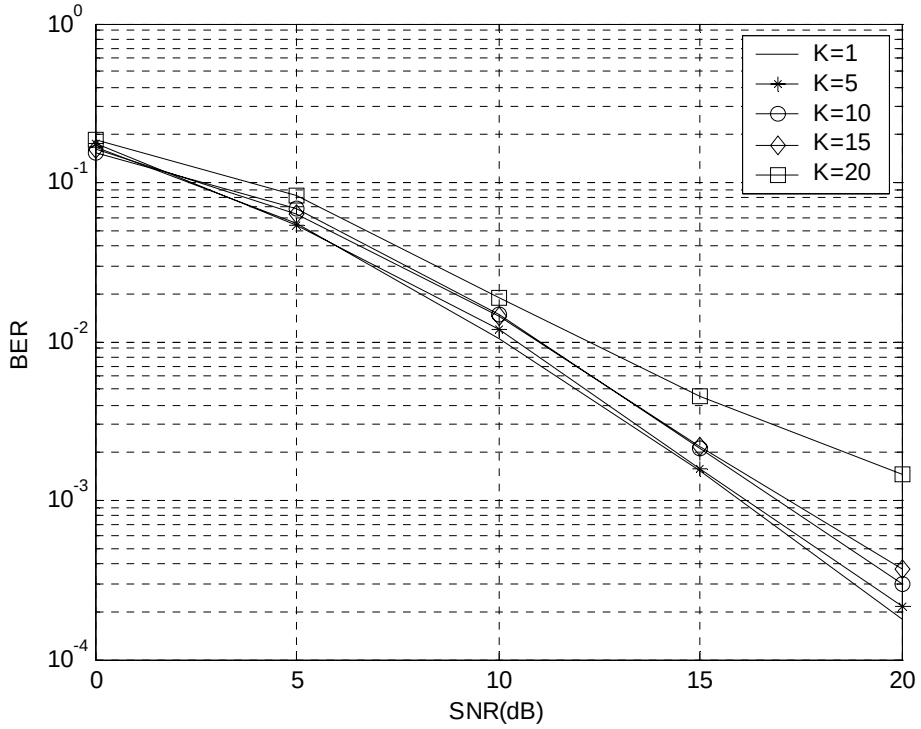

Figure 4.13. The BER of the RSTSIC employing generalized clipper decision function and amplitude averaging for various user loads.

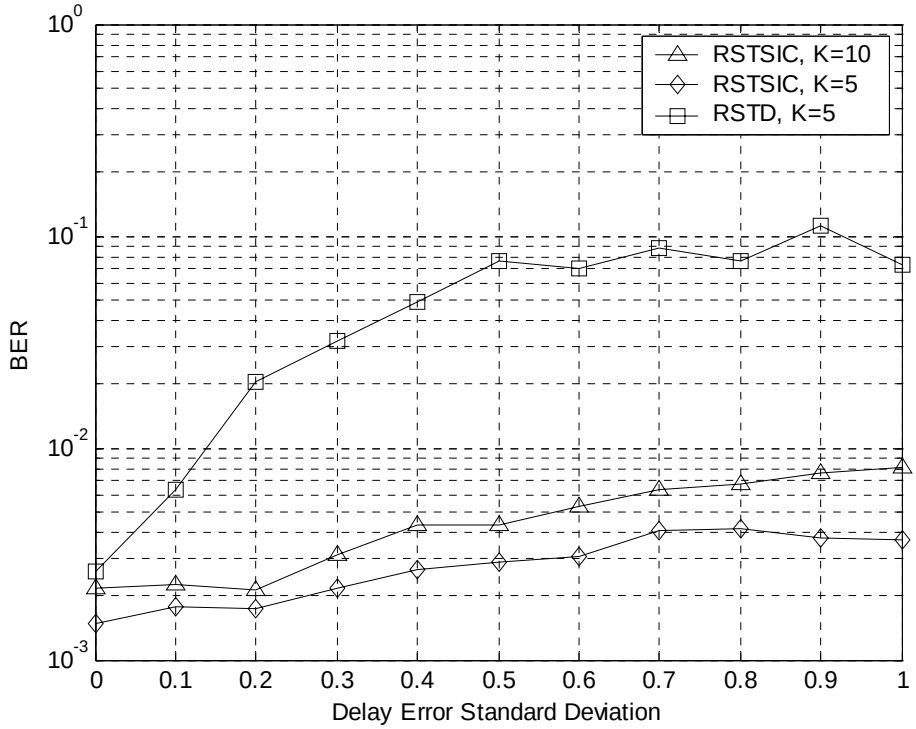

Figure 4.14. The BER as a function of σ_T for the RSTSIC with amplitude averaging and generalized clipper decision function, and the RSTD. The SNR = 15 dB.

The BER performance under various number of antenna elements is shown in Fig. 4.15. The intersection between the curves of the 1x2 and 4x4 systems occurs at a lower SNR value compared to the linear decision function. The quadrupling of the data rate can occur at about 1.5 dB less than the linear decision RSTSIC, which is advantageous in terms of lower power consumption and intercell-interference for the surrounding cells.

Given these results, we see that an enormous BER improvement can be achieved by limiting the amount of noise enhancement and reducing the likelihood of error-propagation, as well as noise variance reduction through amplitude averaging.

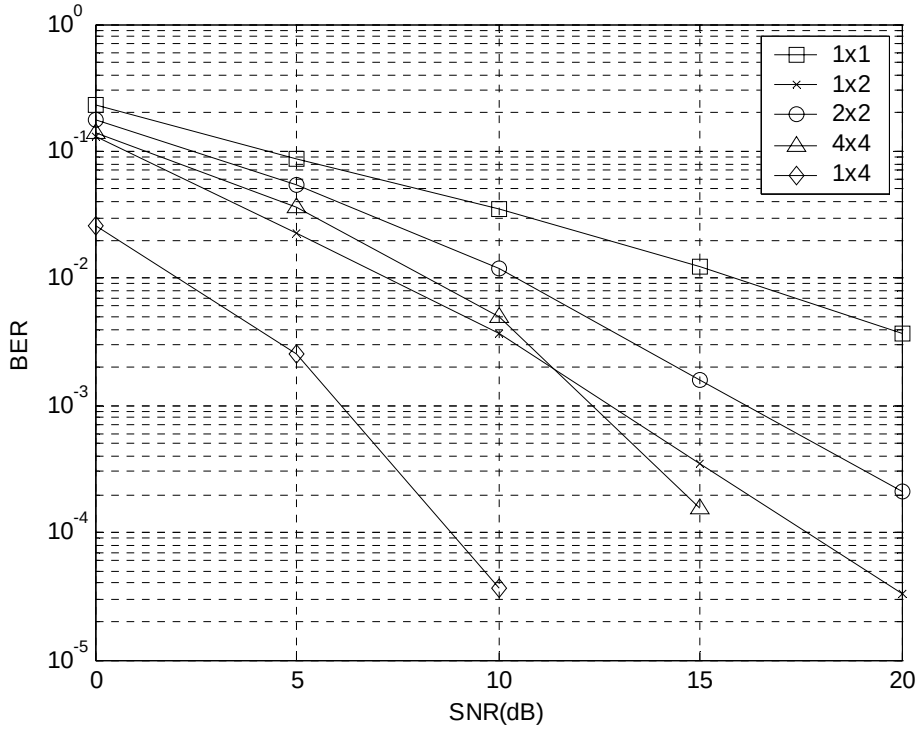

Figure 4.15. Performance under various number of antenna elements of the STDSIC with amplitude averaging and generalized clipper decision function for K = 5 users.

4.9 Performance of the RSTSIC under Zero dB Near-Far Ratio Environment

Throughout the discussions in this chapter, we have assumed a NFR of 20 dB. This is a rather pessimistic scenario of the desired user's environment. In the analysis that follows, we present a more typical scenario where the NFR is 0 dB on average. We let the NFR to be Gaussian distributed with zero-mean and variance of 10. This means that the desired user is no longer the weakest user, but is the median user. Fig. 4.16 shows the performance of the STD and RSTD in the above-mentioned scenario for K = 15 users. The STD with estimated timing is 3 dB worse than the STD with perfect timing information, while the RSTSIC with the generalized clipper decision function is about 0.5 dB worse. There are still performance gains to be made with the

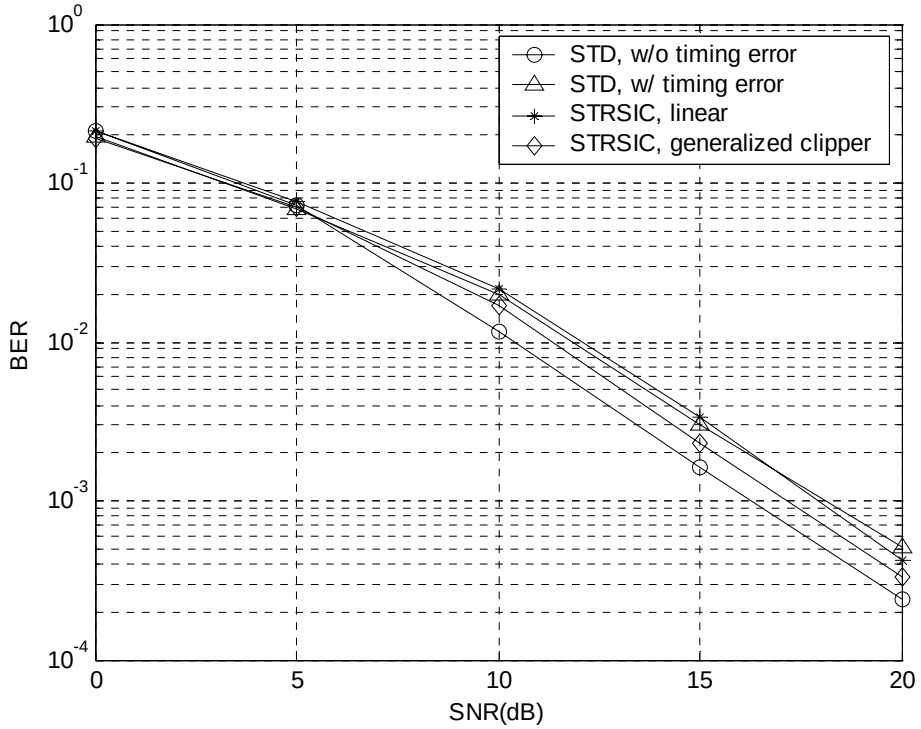

Figure 4.16. Performance comparison of STD and RSTSIC under average near-far ratio of 0 dB. K = 15 users.

RSTSIC, therefore, even when power control is in place.

Chapter 5

Conclusions and Future Work

5.1 Conclusions

In this thesis, a robust SIC is derived for a multiuser CDMA MIMO (MCM) system and its performance is evaluated. The following points summarize the major findings:

1. Time-delay mismatch in a MCM system poses a major impairment on performance. Near-far resistance is destroyed even for the state-of-the-art receivers, rendering them practically useless.
2. The proposed robust space-time SIC (RSTSIC) receiver under timing mismatch is able to achieve performance close to that of the space-time decorrelator (STD) with perfect timing estimates. When amplitude averaging and the generalized clipper decision function are used, the performance gap between RSTSIC and the ideal STD further narrows. In addition, we discover that the capacity is greatly enhanced over that of the linear soft-decision RSTSIC. We note that, however, in a less severe near-far environment as in Section 4.9, performance degradation due to timing mismatch is not as significant. Nevertheless, the RSTSIC can still offer significant performance gain over the STD.

3. In contrast to the single-input single-output robust SIC in [25], the RSTSIC is resistant to large timing estimate errors even without a decorrelating first stage. The RSTSIC BER increases slightly towards the BER ceiling of the robust STD as the standard deviation of the delay estimate error increases.
4. Complexity-wise, the RSTSIC is linear in the number of antennas, users and frame size, whereas the decorrelating and V-BLAST type algorithms are quadratic. For moderate numbers of antenna elements, users and block sizes, the RSTSIC can offer significant complexity reduction.
5. In a rich-scattering channel, data substreams of a particular user should be spread by the same Gold code to maximize spectral efficiency. The scheme of spreading substreams with different random codes is inadequate to facilitate multiuser cancellation due to high cross-correlation between the codes. Moreover, applying distinct Gold codes for different substreams offer little performance improvement.

5.2 Suggestions for Future Work

1. We have assumed perfect estimation of the fading channel at the receiver. It would be of interest to investigate the impact of imperfect estimation of channel gains, as well as methods of channel estimation suitable for the RSTSIC.
2. The flat independently identically distributed fading for the wireless channel is an ideal assumption. Realistically, the multiple artificial channels formed by the antennas arrays will be somewhat correlated in

space. This correlation will hinder the ability of the receiver to separate the substreams of the users spatially, leading to inferior performance.

3. Narrowband CDMA has been implied throughout the thesis as we have considered only single-path channel model. In wideband CDMA, however, multipath will be encountered at the receiver, as the bandwidth of the signal exceeds the coherent bandwidth of the channel. Furthermore, the use of wideband signalling will induce temporally-correlated fading between subsequent transmission frames. Therefore, one should consider modifying the system model to accommodate wideband signalling, and adapting the SIC algorithm accordingly.

Bibliography

[1] K. S. Gilhousen, I. M. Jacobs, R. Padovani, A. J. Viterbi, L. A. Weaver, Jr, and C. E. Wheatley III, "On the capacity of a cellular CDMA system," *IEEE Trans. Vehicular Tech.*, vol. 40, no. 2, pp. 303-311, May 1991.

[2] T. S. Rappaport, A. Annamalai, R. M. Buehrer, and W. H. Tranter, "Wireless communications: past events and a future perspective," *IEEE Commun. Mag.*, pp. 148-161, May 2002.

[3] S. Verdú, "Minimum probability of error for asynchronous Gaussian multiple-access channels," *IEEE Trans. Inform. Theory*, vol. IT-32, pp. 85-96, Jan. 1986.

[4] R. Lupas and S. Verdú, "Near-far resistance of multiuser detectors in asynchronous channels," *IEEE Trans. Commum.*, vol. 38, pp. 496-508, Apr. 1990.

[5] Z. Xie, R. T. Short, and C. K. Rushforth, "A family of suboptimum detectors for coherent multiuser communications," *IEEE J. Select. Areas Commun.*, vol. 4, pp. 683-690, May 1990.

[6] M. K. Varanasi and B. Aazhang, "Multistage detection in asynchronous code-division multiple-access communications," *IEEE Trans. Commun.*, vol. 38, pp. 509-519, Apr. 1990.

[7] P. Patel and J. M. Holtzman, “Analysis of a simple successive interference cancellation scheme in a DS-CDMA system,” *IEEE J. Select. Areas Commun.*, vol. 2, pp. 796-807, June 1994.

[8] R. L. Pickholtz, D. L. Schilling and L. B. Milstein, “Theory of spread-spectrum communications - a tutorial,” *IEEE Trans. Commun.*, vol. 30, no. 5, pp. 855-884, May 1982.

[9] E. G. Ström, S. Parkvall, S. L. Miller and B. E. Ottersten, “Propagation delay estimation in asynchronous direct-sequence code-division multiple access systems,” *IEEE Trans. Commun.*, vol. 44 no. 1, pp. 84-93, Jan. 1996.

[10] S. E. Bensley and B. Aazhang, “Subspace-based channel estimation for code division multiple access communication systems,” *IEEE Trans. Commun.*, vol. 44, no. 8, pp. 1009-1020 Aug. 1996.

[11] J. Joutsensalo, J. Lilleberg, A. Hottinen and J. Karhunen, “A hierarchic maximum likelihood method for delay estimation in CDMA,” *in Proc. VTC’96*, pp. 182-192.

[12] J. Lilleberg, E. Nieminen and M. Latva-Aho, “Blind iterative multiuser delay estimation for CDMA,” *in Proc. PIMRC’96*, pp. 565-568.

[13] U. Madhow, “MMSE interference suppression for timing acquision and demodulation in direct-sequence CDMA systems,” *IEEE Trans. Commun.*, vol. 46, no. 8, pp. 1065-1075, Aug. 1998.

[14] D. Zheng, J. Li, S. L. Miller and E. G. Ström, “An efficient code-timing estimator for DS-CDMA signals,” *IEEE Trans. Signal Process.*, vol. 45, no. 1, pp. 82-89, Jan. 1997.

[15] R. M. Buehrer, A. Kaul, S. Striglis and B. D. Woerner, “Analysis of DS-CDMA parallel interference cancellation with phase and timing errors,” *IEEE J. Select. Areas Commun.*, vol. 14 no. 8, pp. 1522-1534, Oct. 1996.

[16] F. Cheng and J. M. Holtzman, “Effect of tracking error on DS-CDMA successive interference cancellation,” *in Proc. GLOBECOM’94 Mini-Conference*, pp. 166-170.

[17] S. D. Gray, M. Kocic and D. Brady, “Multiuser detection in mismatched multiple-access channels,” *IEEE Trans. Commun.*, vol. 43, no. 12, pp. 3080-3089, Dec. 1995.

[18] K. Kansanen, M. Juntti and M. Latva-Aho, “Performance of parallel interference cancellation receiver with delay errors,” *in Proc. URSI Remote Sensing Club of Finland/IEEE XXXIII Convention on Radio Science and Remote Sensing Symposium*, Epsoo, Finland, pp. 61-62, Aug. 24-25, 1998.

[19] S. Parkvall, E. Ström, and B. Ottersten, “The impact of timing errors on the performance of linear DS-CDMA receivers,” *IEEE J. Selec. Areas Commun.*, vol. 14, pp. 1660-1668, Nov. 1996.

[20] R. Wang, “Spatial-temporal signal processing for multi-user CDMA communication Systems,” Ph.D. Thesis, Queen’s University, 1999.

[21] F. Zheng and S. K. Barton, “On the performance of near-far resistant CDMA detectors in the presence of synchronization errors,” *IEEE Trans. Commun.*, vol. 43, no. 12, pp. 3037-3045, Dec. 1995.

[22] R. A. Iltis, “Demodulation and code acquisition using decorrelator detectors for QS-CDMA,” *IEEE Trans., Commun.*, vol. 44, pp. 1553-1560, Nov. 1996.

[23] F. van Heeswyk, D. D. Falconer and A. U. H. Sheikh, “A delay independent decorrelating detector for quasi-synchronous CDMA,” *IEEE J. Select. Areas Commun.*, vol. 14, pp. 1619-1626, Oct. 1996.

[24] L. Chu and U. Mitra, “Performance analysis of an improved MMSE multiuser receiver for mismatched delay channels,” *IEEE Trans., Commun.*, vol. 46, pp. 1369-1380, Oct. 1998.

[25] W. Zha and S. D. Blostein, “Multiuser Receivers that are robust to delay mismatch,” *IEEE Trans. Commun.*, vol. 50, pp.2072-2081, Dec. 2002.

[26] G. J. Foschini, “Layered space-time architecture for wireless communication in a fading environment when using multi-element antennas,” *Bell Labs Technical Journal*, pp.41-59, Autumn 1996.

[27] H. Huang, H. Viswanathan, and G. J. Foschini, “Multiple Antennas in Cellular CDMA Systems: Transmission, Detection, and Spectral Efficiency,” *IEEE Trans. Wireless Commun.*, vol. 1, pp.383-392, July 2002.

[28] T. Muharemovic, E. N. Onggosanusi, A. G. Dabak, and B. Aazhang, “Hybrid linear-iterative detection algorithms forr MIMO CDMA systems in multipath channels,” in Proc. *IEEE Int. Conf. Acoustics, Speech, and Signal Processing, 2002 (ICASSP '02)*, vol. 3 , pp. 2621-2624, 17 May 2002.

[29] S. Sfar, R. D. Murch and K. B. Letaief, “Layered space-time multiuser detection over wireless uplink systems,” *IEEE Trans. Wireless Commun.*, vol. 2, pp.653-668, July 2003.

[30] A. Duel-Hallen, “A family of multiuser decision-feedback detectors for asynchronous code-division multiple-access channels,” *IEEE Trans. Commun.*, vol. 43, pp. 421-434, Feb./Mar./Apr. 1995.

[31] A. Duel-Hallen, “Equalizers for multiple input multiple output channels and PAM systems with cyclostationary input sequences,” *IEEE J. Selec. Areas Commun.*, vol. 10, pp. 630-639, Apr. 1992.

[32] L. K. Rasmussen, T. J. Lim, and A. Johansson, “A matrix-algebraic approach to successive interference cancellation in CDMA,” *IEEE Trans. Commun.*, vol. 48, pp. 145-151, Jan. 2000.

[33] G. J. Foschini, G. D. Golden, R. A. Valenzuela and P. W. Wolniansky, “Simplified Processing for high spectral efficiency wireless communication employing multi-element arrays,” *IEEE J. Selec. Areas Commun.*, vol. 17, no. 3, pp. 1841-1852, Nov. 1999.

[34] V. Tarokh, N. Seshadri, and A. R. Calderbank, “Space-time codes for high data rate wireless communications: Performance criterion and code construction,” *IEEE Trans. Inform. Theory*, vol. 44, pp. 744-765, Mar. 1998.

[35] B. Hochwald, T. Marzetta and C. Papadias, “A transmitter diversity scheme for wideband CDMA systems based on space-time spreading,” *IEEE J. Selec. Areas Commun.*, vol. 19, no. 1, pp. 48-60, Jan. 2001.

[36] M. Varanasi, “Group detection for synchronous CDMA systems,” *IEEE Trans. Inform. Theory*, vol 41, pp. 1083-1096, July 1995.

[37] J. Shen and Z. Ding, “Edge decision-assisted decorrelators for asynchronous CDMA channels,” *IEEE Trans. Commun.*, vol. 47, pp. 438-445, Mar. 1999.

[38] F. Zheng and S. K. Barton, “Near-far resistant detection of CDMA signals via isolation bit insertion,” *IEEE Trans Commun.*, vol. 43, pp.1313-1317, Apr. 1995.

[39] J. A. Fessler and A. O. Hero, “Space-alternating generalized expectation-maximization algorithm,” *IEEE Trans. Signal Processing*, vol. 42, pp. 2664-2677, Oct. 1994.

[40] R. Wang and S. D. Blostein, “A spatial-temporal decorrelating receiver for CDMA systems with base-station antenna arrays,” *IEEE Trans. Commun.*, vol. 49, pp. 329-340, Feb. 2001.

[41] P. Patel and J. M. Holtzman, “Analysis of a simple successive interference cancellation scheme in a DS-CDMA system,” *IEEE J. Select. Areas Commun.*, vol. 14, no. 8, pp. 1660-1668, June 1996.

[42] L. B. Nelson and H. V. Poor, “Iterative multiuser receivers for CDMA channels: an EM-based approach,” *IEEE Trans. Commun.*, vol. 44, no. 12, pp. 1700-1710, Dec. 1996.

[43] W. Zha and S. D. Blostein, “Soft-decision multistage multiuser interference cancellation,” *IEEE Trans. Veh. Tech.*, vol. 52, no. 2, pp.380-389, Mar. 2003.

[44] S. Verdu, *Multiuser Detection*. New York: Cambridge Univ., 1998.

[45] J. G. Proakis, Digital Communications. New York : McGraw-Hill, 2001.

[46] A. Wittneben, “A new bandwidth efficient transmit antenna modulation diversity scheme for linear digital modulation,” *in Proc. IEEE Int. Conf. Communications*, pp. 1630–1634, 1993.

[47] S. M. Alamouti, “A simple transmitter diversity scheme for wireless communications,” *IEEE J. Selec. Areas Commun.*, vol. 16, pp. 1451-1458, Oct. 1995.

[48] K. Sheikh, D. Gesbert, D. Gore, and A. Paulraj, “Smart Antennas for Broadband wireless access networks,” *IEEE Commun., Mag.*, vol 37, pp. 100-106, Nov. 1999.

Appendix A

Matlab Code of the Robust Space-Time SIC

This Matlab program simulates the BER of the RSTSIC for a 2x2 MCM System

```
%%%%%%%%%%%%
%% Parameters set up
%%%%%%%%%%%%

K=5;                % number of users in the system
N1=2;               % number of transmit antennas
N2=2;               % number of receive antennas
L=31;               % length of PN spreading code
M=4;                % number of bits in a frame transmission
delay_dev=0.1;      % standard deviation of delay error distribution

NF_db_ratio=20;             % Near-Far ratio in dB
SNR_db_set=0:5:20;          % specify SNR range in dB.

monte_num=2500;             % number of monte carlo simulations for given a SNR

%%%%%%%%%%%%
%% Simulations
%%%%%%%%%%%%

SNR_index=0;
randn('state',sum(100*clock))
```

```
for SNR_db=SNR_db_set

  Ps=1;                          % unit transmission power of desired user
  Pi=Ps*10^(NF_db_ratio/10);     % interference power defined by the near-far ratio
  No=10^(-SNR_db/10);            % noise power

  SNR_index=SNR_index+1;         % increment SNR to the next defined value

  corr=0;                        % number of correctly detected bits for RSTSIC

  %---------------
  % Monte Carlo
  %---------------

  for num=1:monte_num            % Monte Carlo loop

     %%%%%%%%%%%%%%%%%%%%%%%%%%%
     %% generate i.i.d. flat fading MIMO channel Matrix
     %%%%%%%%%%%%%%%%%%%%%%%%%%%

     %%% independent channel
     C=(randn(N2,N1)+i*randn(N2,N1))/sqrt(2);

     I=eye(K*M);
     c1=diag(C(1,:));            % channel matrix from Eq. (3.6)
     c2=diag(C(2,:));
     C1=kron(I,c1);              % block-diagonal channel matrix from Eq. (3.5)
     C2=kron(I,c2);

     H1=c1'*c1;                  % used for normalization in Eq. (3.27)
     H2=c2'*c2;

     %%%%%%%%%%%%%%%%%
     %% generate timing parameters
     %%%%%%%%%%%%%%%%%

     for ii=1:N1*N2
        % independent Gaussian random variable for fractional part of delay
        temp=rand;
        offset_frac(ii,1)=temp;
     end;

     for ii=1:N1*N2
        % independent uniform random variable for interger part of delay
        temp=L*rand;
        offset_int(ii,1)=fix(temp);
```

```
end;

% concatenate delay error to within 0.5 T_C
for ii=1:N1*N2
   temp=randn*delay_dev;
   if temp>0.5
      temp=0.5;
   elseif temp<-0.5
      temp=-0.5;
   end;

% change sign of delay est. error to ensure timing estimation is within the same chip
   if offset_frac(ii,1)+temp >= 1.0
      offset_est(ii,1)=offset_frac(ii,1)-temp;
   elseif offset_frac(ii,1)+temp < 0.0
      offset_est(ii,1)=offset_frac(ii,1)-temp;
   else
      offset_est(ii,1)=offset_frac(ii,1)+temp;
   end;
end;

%%%%%%%%%%%%%%%%%
%% generate the data bit vector
%%%%%%%%%%%%%%%%%

% bit vector in Eq. (3.8)
for ii=1:K*N1*M
   temp=rand;
   if temp < 0.5
      B(ii,1)=-1;
   else
      B(ii,1)=1;
   end;
end;

%%%%%%%%%%%%%%%%%
%% generate amplitude matrix
%%%%%%%%%%%%%%%%%

% set up amplitude diagonal matrix from Eq. (3.7)
a(1:N2,1)=Ps;
if K>1
   a(N2+1:N2*2,1)=Pi;
   if K>2
      for ii=3:K
         a(N2*2+(ii-3)*N2+1:N2*2+(ii-2)*N2,1)=Pi-(ii-2)*(Pi-Ps)/(K-1);
```

```
      end;
   end;
end;
I=eye(M);

aa=sqrt(diag(a));
A=kron(I,aa);

%%%%%%%%%%%%%%%%%%
%% generate PN code for each user
%%%%%%%%%%%%%%%%%%

% Gold code of length 31 is used here
GC=goldcode(L,K);
c=zeros((M+1)*L,K);
c(1:L,1:K)=GC(:,1:K);

% S1 and S2 are true spreading code matrices
% dc1 and dc2 are estimated spreading code matrices
% dd1 and dd2 are error code matrices
for ii=1:K
for nn=1:N2
for jj=1:M
    S1(:,(jj-1)*K*N2+nn+(ii-1)*N2)=offset_frac(nn).*wshift('1D',c(:,ii),-((jj-
        1)*L+offset_int(nn)+1))+(1-offset_frac(nn)).*wshift('1D',c(:,ii),-((jj-
        1)*L+offset_int(nn)));
    S2(:,(jj-1)*K*N2+nn+(ii-1)*N2)=offset_frac(nn+N2).*wshift('1D',c(:,ii),-((jj-
        1)*L+offset_int(nn+N2)+1))+(1-offset_frac(nn+N2)).*wshift('1D',c(:,ii),-((jj-
        1)*L+offset_int(nn+N2)));
    dc1(:,(jj-1)*K*N2+nn+(ii-1)*N2)=offset_est(nn).*wshift('1D',c(:,ii),-((jj-
        1)*L+offset_int(nn)+1))+(1-offset_est(nn)).*wshift('1D',c(:,ii),-((jj-
        1)*L+offset_int(nn)));
    dd1(:,(jj-1)*K*N2+nn+(ii-1)*N2)=wshift('1D',c(:,ii),-((jj-
        1)*L+offset_int(nn)+1))-wshift('1D',c(:,ii),-((jj-1)*L+offset_int(nn)));
    dc2(:,(jj-1)*K*N2+nn+(ii-1)*N2)=offset_est(nn+N2).*wshift('1D',c(:,ii),-((jj-
        1)*L+offset_int(nn+N2)+1))+(1-offset_est(nn+N2)).*wshift('1D',c(:,ii),-((jj-
        1)*L+offset_int(nn+N2)));
    dd2(:,(jj-1)*K*N2+nn+(ii-1)*N2)=wshift('1D',c(:,ii),-((jj-
        1)*L+offset_int(nn+N2)+1))-wshift('1D',c(:,ii),-((jj-1)*L+offset_int(nn+N2)));
end;
end;
end;
```

```
%%%%%%%%%%%%%%%%%%
%% generate noise & observations
%%%%%%%%%%%%%%%%%%

% form received vector for each antenna in Eq. (3.3)

noise1=sqrt(No)*(randn(L*(M+1),1)+i*randn((M+1)*L,1))/sqrt(2);
noise2=sqrt(No)*(randn((M+1)*L,1)+i*randn((M+1)*L,1))/sqrt(2);

r1=S1*C1*A*B+noise1;
r2=S2*C2*A*B+noise2;

%%%%%%%%%%
%% SIC initialization
%%%%%%%%%%

ac=zeros(M,K*N1);              % est. amplitudes
bc=zeros(M,K*N1);              % est. bits
adc1=zeros(K,N1);              % amplitudes of error vectors
adc2=zeros(K,N1);
e1=zeros((M+1)*L,K*N1);        % error vectors
e2=zeros((M+1)*L,K*N1);

%%%%%%%%%%
%% SIC iteration steps
%%%%%%%%%%

stages=15;      % max. num. of stages for SIC
threshold=0;   % number of est. amp. that are within 1% of previous est. amp.

while ((stages>0)&(threshold<K*M*N1))

for kk=1:K
for nn=1:N1

% estimate user kk's nnth substreams' signal amplitudes and data bits
for jj=1:M

    % next three steps performs Eq. (3.26)
    d_norm = dc1(:,(jj-1)*K*N1+(kk-1)*N1+nn)'*dc1(:,(jj-1)*K*N1+(kk-1)*N1+nn);
    newInfo1(jj) = real(c1(nn,nn)'*dc1(:,(jj-1)*K*N1+(kk-1)*N1+nn)'*r1);
    newInfo1(jj) = newInfo1(jj)/d_norm; % normalize

    d_norm = dc2(:,(jj-1)*K*N1+(kk-1)*N1+nn)'*dc2(:,(jj-1)*K*N1+(kk-1)*N1+nn);
    newInfo2(jj) = real(c2(nn,nn)'*dc2(:,(jj-1)*K*N1+(kk-1)*N1+nn)'*r2);
    newInfo2(jj) = newInfo2(jj)/d_norm; % normalize
```

```
    % next two steps perform Eq. (3.27)
    newInfo(jj)=(newInfo1(jj)+newInfo2(jj))/2;
    newInfo(jj)=newInfo(jj)/((H1(nn,nn)+H2(nn,nn))/2);

    % save value of previous est. amplitude for exit condition
    acprev(jj,(kk-1)*N1+nn)=ac(jj,(kk-1)*N1+nn);

    % new plus old info
    temp3=newInfo(jj) + ac(jj,(kk-1)*N1+nn)*bc(jj,(kk-1)*N1+nn);
    ac(jj,(kk-1)*N1+nn)=abs(temp3);      % Eq. (3.28)
    bc(jj,(kk-1)*N1+nn)=sign(temp3);     % Eq. (3.29)
end;

%%% update user kk's reconstructed signal using Eq. (3.30)

rc1(:,(kk-1)*N1+nn)=zeros((M+1)*L,1);
rc2(:,(kk-1)*N1+nn)=zeros((M+1)*L,1);

for jj=1:M
% only sum the new information
rc1(:,(kk-1)*N1+nn)=rc1(:,(kk-1)*N1+nn)+c1(nn,nn)*newInfo(jj)*dc1(:,(jj-
    1)*K*N1+(kk-1)*N1+nn);
rc2(:,(kk-1)*N1+nn)=rc2(:,(kk-1)*N1+nn)+c2(nn,nn)*newInfo(jj)*dc2(:,(jj-
    1)*K*N1+(kk-1)*N1+nn);
end;

% subtract to cancel the new information (onion-peeling)
r1=r1-rc1(:,(kk-1)*N1+nn);
r2=r2-rc2(:,(kk-1)*N1+nn);

%%% estimate residual signal of the kth user
% first add back the error signal for this user

r1=r1+c1(nn,nn)*adc1(kk,nn)*e1(:,(kk-1)*N1+nn);
r2=r2+c2(nn,nn)*adc2(kk,nn)*e2(:,(kk-1)*N1+nn);

%%% update amplitude of error vector using Eq. (3.32) and (3.33)

e1(:,(kk-1)*N1+nn)=zeros((M+1)*L,1);
e2(:,(kk-1)*N1+nn)=zeros((M+1)*L,1);

for jj=1:M
e1(:,(kk-1)*N1+nn)=e1(:,(kk-1)*N1+nn)+dd1(:,(jj-1)*K*N1+(kk-
    1)*N1+nn)*bc(jj,(kk-1)*N1+nn);
e2(:,(kk-1)*N1+nn)=e2(:,(kk-1)*N1+nn)+dd2(:,(jj-1)*K*N1+(kk-
    1)*N1+nn)*bc(jj,(kk-1)*N1+nn);
```

```
        end;

    e_norm=e1(:,(kk-1)*N1+nn)'*e1(:,(kk-1)*N1+nn);
    adc1(kk,nn)=real(c1(nn,nn)'*e1(:,(kk-1)*N1+nn)'*r1);
    adc1(kk,nn)=adc1(kk,nn)/e_norm/H1(nn,nn);   % normalize

    e_norm=e2(:,(kk-1)*N1+nn)'*e2(:,(kk-1)*N1+nn);
    adc2(kk,nn)=real(c2(nn,nn)'*e2(:,(kk-1)*N1+nn)'*r2);
    adc2(kk,nn)=adc2(kk,nn)/e_norm/H2(nn,nn);   % normalize

    % then subtract the newly estimated error signal, performing Eq. (3.34)
    r1=r1-c1(nn,nn)*adc1(kk,nn)*e1(:,(kk-1)*N1+nn);
    2=r2-c2(nn,nn)*adc2(kk,nn)*e2(:,(kk-1)*N1+nn);

    end; % end for (stream 1:N1)
    end; % end for (users 1:K)

    %%% check for loop exit condition

    stages=stages-1;
    threshhold=0;

    for jj=1:M
    for ii=1:K*N1
        %checking amplitude changes for all users and substreams
        if abs(ac(jj,ii)-acprev(jj,ii))<0.01
                threshold=threshold+1;
        end;
    end;
    end;

    end; % end while (SIC iterations) loop

    %%%%%%%%%%%%%%%%%%%%
    %% check for correct bit detection
    %%%%%%%%%%%%%%%%%%%%

    for nn=1:N1
        for jj=1:M
                if bc(jj,nn)==B((jj-1)*K*N1+nn)
                        corr=corr+1;
                end;
        end;
    end;

end; % end of monte carlo
```

```
%%% calculate average BER
avg_ber(SNR_index)=1-corr/monte_num/N1/M

end; % end of SNR_index
```

Vita

Robert Chao Yung Lu

Education

2001-Present	Candidate for Master of Science in Electrical Engineering Queen's University Kingston, Ontario
1997-2001	Bachelor of Applied Science in Electrical Engineering Computer Option Queen's University Kingston, Ontario

Work Experience

2001 - 2003	Research Assistant Department of Electrical and Computer Engineering Queen's University
2001 - 2003	Teaching Assistant Department of Electrical and Computer Engineering- Queen's University
2000 - 2001	Research Assistant Department of Electrical and Computer Engineering Queen's University
1998 - 1999	Network Support Information Technology Services Queen's University

1998 July-Aug.	Project Leader Numbertel Inc. Toronto, Ontario
1997 July-Aug.	Project Assistant Numbertel Inc Toronto, Ontario

Awards

2001-2003	Queen's Graduate Award

Poster Presentation

R. C. Y. Lu, S. D. Blostein, "Robust-to-timing multiuser detector for CDMA MIMO systems," at *Bell University Labs Conference*, Toronto, Canada, Nov. 17, 2003.